LA-5328-MS

INFORMAL REPORT

C.3

Heat Transfer and Chemical Stability Calculations for Controlled Thermonuclear Reactors (CTR)

los alamos
scientific laboratory
of the University of California
LOS ALAMOS, NEW MEXICO 87544

UNITED STATES
ATOMIC ENERGY COMMISSION
CONTRACT W-7405-ENG. 36

LA-5328-MS
INFORMAL REPORT
SPECIAL DISTRIBUTION
ISSUED: July 1973

los alamos
scientific laboratory
of the University of California
LOS ALAMOS, NEW MEXICO 87544

Heat Transfer and Chemical Stability Calculations for Controlled Thermonuclear Reactors (CTR)

by

J. W. Tester*
R. C. Feber
C. C. Herrick

*Visiting Staff Member. Permanent address: Oak Ridge National Laboratory, M.I.T. Station, Oak Ridge, TN 37830.

HEAT TRANSFER AND CHEMICAL STABILITY CALCULATIONS FOR CONTROLLED THERMONUCLEAR REACTORS (CTR)

by

J. W. Tester
R. C. Feber
C. C. Herrick

ABSTRACT

Both heat transfer characteristics and chemical stabilities of several proposed first-wall materials including Nb, Al_2O_3, and Mo were examined over a range of conceivable operating conditions for a pulsed high beta machine. Heat fluxes from .1 to 10 kW/cm^2 were considered for .1 to 1 cm wall thicknesses. With an incident Bremsstrahlung flux of (10 kW/cm^2) and a 10% duty cycle, none of the materials proposed looked feasible. By decreasing the Bremsstrahlung flux to (1 kW/cm^2) with a 10% duty cycle, a 1 mm Al_2O_3 wall attains steady state conditions at ~1000°C. Chemical stabilities of Al_2O_3, BeO, and BN, were examined in molecular and atomic hydrogen environments. The materials are satisfactory in molecular hydrogen at 827°C, show modest reaction at 1227°C, and are unsuitable at 1727°C. In a hydrogen atom environment, over a pressure range of 1×10^{-5} to 10 torr, all selected materials were unsatisfactory.

SUMMARY

Two major problems are anticipated with fusion reactor first wall materials: (1) excessive wall surface heating caused by the deposition of large quantities of heat, 1-10 kW/cm^2, and (2) chemical erosion of the wall caused by plasma fuel particles bombarding the inner surface. Heat transfer and chemical stability characteristics were analyzed for several proposed first wall materials, viz Nb, Mo, Al_2O_3, BeO, BN, and SiC.

Heat conduction through the wall was treated numerically as a one-dimensional, unsteady state problem incorporating an appropriate liquid metal heat transfer coefficient for the lithium blanket. The inner wall surface was modeled by specifying the heat flux, primarily Bremsstrahlung radiation, during the pulse. In this preliminary analysis the heat conducted to the inner surface during the rest cycle was neglected.

The pulse time was specified as 0.01 sec with a rest period of 0.09 sec to simulate proposed Z-pinch operating conditions. The effects of material thermal properties were examined by calculating steady state temperature profiles as a function of incident heat flux ~ (.1-10 kW/cm^2), wall thickness (0.1 - 1.0 cm), and liquid metal heat transfer coefficient (0.14 - 14 cal/cm^2-sec-°C). Thermal diffusivities (cm^2/sec) of 1.117 for Cu, 0.545 for Mo, 0.250 for Nb, and 0.0434 for Al_2O_3 provided a significant range of thermal properties. With an incident heat flux of ~10 kW/cm^2, 800°C ambient Li, and a 10% duty cycle, none of the proposed materials

looked feasible since the surface temperature exceeded the melting point after several pulses. At lower heat fluxes, ~ 1 kW/cm^2, a 0.1 cm Al_2O_3 wall attained steady state conditions at 1000°C which is approximately half of the melting temperature.

Apart from the serious implications of the heat transfer analysis, chemical erosion problems present some potential problems. Chemical stabilities of solid Al_2O_3, BeO, BN, and SiC were examined in atomic and molecular hydrogen over temperatures from 827°C to 1727°C and partial pressures from 1 to 10 Torr. Chemical equilibrium was assumed as a limiting criteria, and free energies were minimized numerically to obtain equilibrium compositions. For most cases, the proposed materials were unsuitable unless very small reaction probability values exist to avoid excessive decomposition.

The heat transfer dilemma can be approached in several ways. Since dielectric materials such as Al_2O_3 are desirable but possess poor thermal conductivities, a method currently under investigation is to enhance poor thermal properties by incorporating ordered lattice defects. Should this prove to be unsuccessful, serious consideration should be given to both radial and circumferentially layered composites. The thermal effectiveness of any proposed composite could be analyzed with minor alteration of the existing finite difference code.

The potential chemical stability problem should be confirmed by laboratory experiments. If confirmed, the problem may be handled by employing a radial layered composite or if a circumferentially layered composite is chosen by replenishment "in situ" using a suitable purge gas. Chemical stabilities of suggested materials can be analyzed with the present code.

INTRODUCTION AND SCOPE

This preliminary report concerns first-wall material problems associated with controlled thermo nuclear reactors (CTRs). Material choices for the first wall are limited.[1,2] A typical first wall material must be inert to liquid lithium, capable of withstanding large bremmstrahlung and neutron fluxes, possess good dielectric properties and conduct heat well with no chemical or evaporative deterioration at 1000°C and higher in the presence of a deuterium-tritium gas mixture. Specific radiation damage effects such as swelling and embrittlement were reflected in our treatment.

Numerical values of most, if not all, of the design parameters are uncertain. For present purposes, the pulsed machine is designed for a 10% duty cycle, e.g., a pulse time, τ_p of 0.01 sec followed by a rest time, τ_r, of 0.09 sec. Surface heat fluxes were varied from .1 to 10 kW/cm^2 to examine their effect on the inside surface temperature for various wall thicknesses.

Incident flux on the first wall surface is primarily bremsstrahlung radiation of average wavelength 0.25 Å. The absorption distance into the wall varies with atomic number, e.g., 60% of 15 to 38 Kev bremsstrahlung energy is absorbed in 0.1 cm of Al_2O_3, whereas complete absorption occurs in less than 0.01 cm of Nb.[3] Neutron deposition energy in the wall is assumed to be insignificant relative to the bremsstralung flux. The plasma cooling heat dump during the rest cycle is undoubtedly very important but was ignored in this analysis.[3]

Since a molten lithium blanket surrounding the plasma will be used for cooling as well as tritium breeding, heat transfer effects on the outside of the first wall are secondary, and the temperature profile in the wall will be controlled by the rate of heat conduction through it. To improve the thermodynamic efficiency of the CTR in producing usable power, a maximum liquid lithium temperature of 800°C should be used in the primary heat exchange step.

During the rest cycle, the expanding plasma fuel will consist mostly of a deuterium-tritium mixture which could interact chemically with the wall at surface temperatures. Since the wall must remain stable to bombardment by reducing plasma, chemical reactions and evaporation effects were also examined.

Heat transfer and chemical stability characteristics are considered separately in this report for a number of materials including copper, niobium, molybdenum, alumina, beryllia, and boron nitride.

Heat Transfer Analysis at the First Wall

Preliminary work in this area has been reported by Ribe and associates[3] as well as Phillips and colleagues.[4] Temperature profiles and surface temperature variations were examined under pulsed and continuous heating conditions. The effects of incident heat flux, internal heat production, liquid lithium heat transfer, and wall thickness were studied for copper, niobium, alumina, and molybdenum to provide a range of thermal properties.

Heat transfer through the wall is approximated by a one-dimensional, unsteady-state system. A numerical, finite difference technique was used to solve the heat conduction equation with heat generation:

$$\alpha \frac{\partial^2 T}{\partial x^2} = \frac{\partial T}{\partial t} + \frac{C}{k} \qquad (1)$$

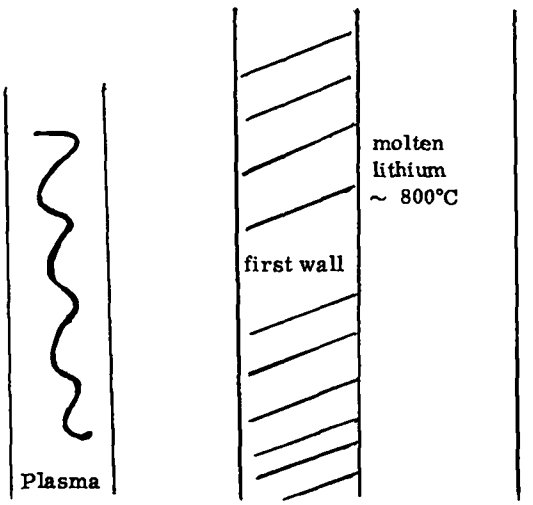

Associated boundary conditions are:

(1) at x = 0 (outside wall), a specified heat flux is given by the heat transfer coefficient, h (cal/cm^2-sec-°C),

$$k\left(\frac{\partial T}{\partial x}\right)_{x=0} = h\,(T - T_B). \qquad (2)$$

(2) at x = ℓ (inside wall), a periodic boundary condition accounts for bremsstralung pulsing. For this preliminary treatment, all thebremsstrahlung is assumed to be deposited on the surface (x = ℓ)

$$k\frac{\partial T}{\partial x}\Big)_{x=\ell} = \begin{cases} Q_i & i(\tau_r + \tau_p) < t < i(\tau_r + \tau_p) + \tau_p \\ 0 & i(\tau_r + \tau_p) + \tau_p < t < (i+1)(\tau_r + \tau_p) \end{cases} \qquad (3)$$

$$i = 0, 1, 2, \ldots.$$

Where:

C = heat generation rate = cal/sec cm^3
h = heat transfer coefficient (liquid Li), cal/cm^2-sec-°C
k = thermal conductivity, cal/cm^2-sec-°C/cm
ℓ = wall thickness, cm
T = wall temperature at x and t, °C
t = time, sec
T_B = bulk Li temperature ~800°C
x = distance, cm
α = thermal diffusivity = $\frac{k}{\rho C_p}$, cm^2/sec
ρ = density, g/cm^3
C_p = heat capacity, cal/g-°C
τ_p = pulse time, sec
τ_r = rest time, sec
Q_i = flux, cal/cm^2-sec

A numerical technique was selected (see Appendix A) for its convenience. Should the heat generation or the thermal diffusivity terms be functions of time, temperature, and/or wall position, their inclusion becomes less difficult in a numerical method than modification of existing analytical solutions. The wall, of thickness ℓ , was divided into 100 equal sized intervals with time increments Δt, selected to satisfy the stability criteria that $\alpha \Delta t / \Delta x^2 < 0.5$ (see Appendix A).

RESULTS

Continuous Heating

Analysis of the continous heating case was accomplished by revising boundary #2 and solving Eq. (1) numerically using the property values given in Table I. A flux of 2382 cal/cm^2-sec ≈(10 kW/cm^2) for 0.01 sec produces surface temperature rises given in Table II for Cu, Mo, Nb, and Al_2O_3. These results compare favorably with those of Phillips et al[2] which were obtained from an analytical solution of a semi-infinite solid model where T was directly proportional to Q_i and $\sqrt{t}$. Thus, the temperature

TABLE I

MATERIAL PROPERTIES (a)

Material	k cal/cm^{2}sec K/cm	ϱ g/cm^3	C_p cal/g K	$\alpha = k/\varrho C_p$ cm^2/sec
Cu - Copper	.91	8.92	.0915	1.117
Al_2O_3 - Alumina	.034	3.96	.198	.0434
Mo - Molybdenum	.350	10.20	.0630	.545
Nb - Niobium	.158	8.57	.0736	.250

k - thermal conductivity

ϱ - density

C_p - heat capacity

α - thermal diffusivity

(a) data based on information taken at ~ 800°C from

1. Perry's Handbook for Chemical Engineers., Fourth Edition
2. Handbook of Chemistry and Physics
3. Thermal Conductivity Handbook

TABLE II

SUMMARY OF RESULTS FROM CONTINUOUS CASE

$Q_{incident}$ = 2382 cal/cm^2-sec (10 kW/cm^2)

$H_{generation}$ = 0

total time elapsed = 10,000 μ sec = 0.01 sec

Material	$\Delta T = T_S - T_B$ (°C)	T_S (°C)	T_M (°C)	T_T (°C)
Cu	322.9	1122.9	1084	542
Mo	577.0	1377.0	2620	1310
Nb	922.9	1722.9	2470	1235
Al_2O_3	1727.0	2527.0	2015	1008

T_M = melting temperature

T_S = surface temperature inside of the first wall

T_B = bulk temperature of the lithium = 800°C

T_T = homologous temperature = $\frac{1}{2}T_M$

h = 14 cal/cm^2-sec-°C

rise for other wall fluxes for the same heating period can be approximated by using a ratio of Q_i's e.g. for a 1 kW/cm^2 loading on Al_2O_3 at .01 sec, $\Delta T \cong 173°C$. (See Table 2).

Pulsed Heating

The basic phenomena of operating a pulsed machine is given by the temperature profiles taken over a 0.1-sec cycle and illustrated in Fig. 1. An incident flux of 238.2 cal/cm^2-sec ~ (1 kW/cm^2) at a 1 cm Al_2O_3 wall was used. Each of the ten lines represents a 0.01-sec interval. Following the first pulse the profile is drawn to a maximum ΔT of 190°C at $x/\ell = 1$. During the first rest period this temperature decays to a value near 30°C since the heat dump is excluded from these calculations. The next pulse produces a higher surface temperature as its initiation commences from the T_B + 30°C value. This process continues until a steady state temperature distribution is attained.

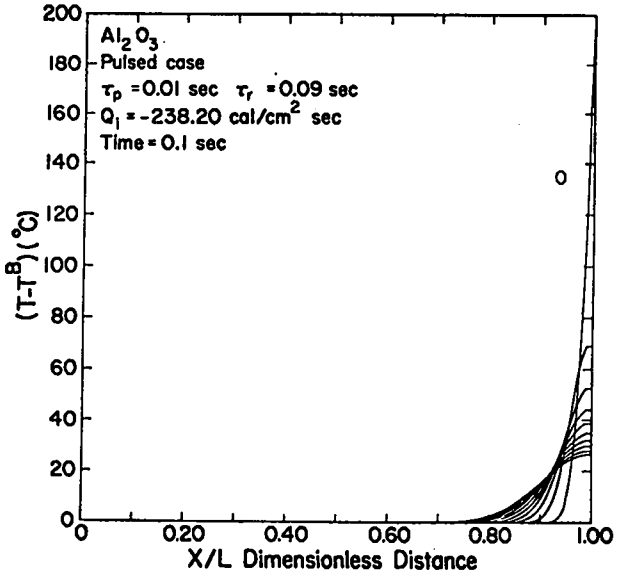

Fig. 1. Temperature profiles in a 1 cm thick Al_2O_3 wall with an incident flux of 238.2 cal/cm^2 (1 kW/cm^2). Each line represents .01 sec of elapsed time. Line 0 is just after the 1st pulse.

Should the incident flux be increased to 1191 or 2382 cal/cm^2-sec $\approx$ (5 or 10 kW/cm^2) retaining a 0.01-sec pulse duration, a significant surface temperature rise occurs as Fig. 2 illustrates. Curves are plotted after each pulse until a running time of 2.21 sec (22 pulses) has elapsed. Here ΔT_S exceeds 1000°C or T wall > 1800°C (T_B = 800°C) thereby creating serious problems with Al_2O_3.

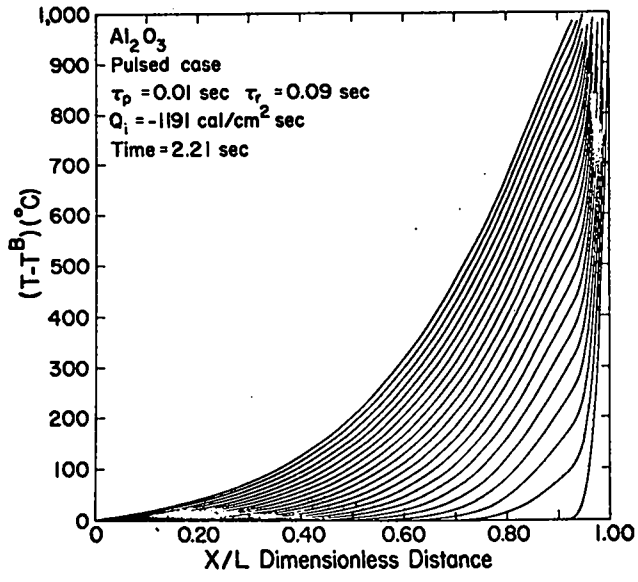

Fig. 2. Temperature profiles in a 1 cm thick Al_2O_3 wall with an incident flux of 1191 cal/cm^2 sec (5 kW/cm^2). Each line is drawn at the end of every pulse.

Profiles similar to those of Fig. 1 occur for Cu as shown in Fig. 3. Copper's thermal conductivity is 0.91 cal/cm^2-sec-°C/cm versus 0.034 cal/cm^2-sec-°C/cm for Al_2O_3; this permits a Cu wall to tolerate higher incident fluxes, viz. Q_i = 10 kW/cm^2 with only a 320°C rise following the first pulse.

Continuous pulsing at a Cu wall yields the temperature distribution shown in Fig. 4. After 4.51 sec or 46 pulses the temperature rise at the inside surface has reached ~530°C. Addition of these temperature rises to the 800°C bulk value means the inside surface of the copper wall melted during the first pulse. Mechanical strength problems with a material generally start at half the melting temperature.

Figures 5 and 6 illustrate similar behavior with Nb which has thermal properties intermediate between Al_2O_3 and Cu. As expected, the temperature excursion with Nb at 238.2 cal/cm^2-sec $\approx$ (1 kW/cm^2) loading is considerably less than with Al_2O_3.

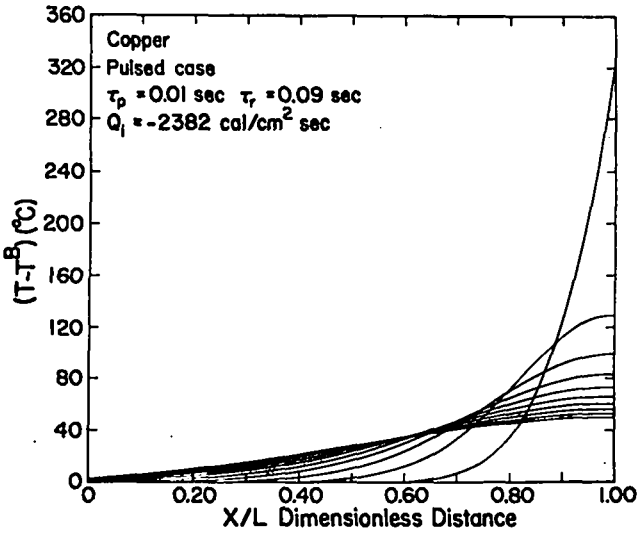

Fig. 3. Temperature profiles in a 1 cm thick Copper wall with an incident flux of 2382 cal/cm^2 sec (10 kW/cm^2). Each line represents .01 sec of elapsed time.

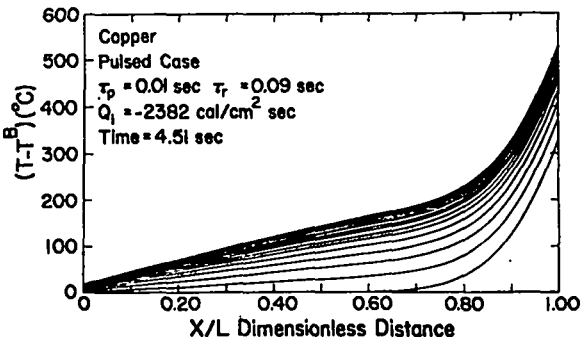

Fig. 4. Temperature profiles in a 1 cm thick Copper wall with an incident flux of 2382 cal/cm^2 sec (10 kW/cm^2). Approach to steady state temperature distribution after 46 pulses with each line appearing at the end of every pulse. (Δt = .10 sec)

An alternative to reducing the wall flux would be to lower the bulk temperature from 800°C. This, of course, would have the disadvantage that lower thermodynamic conversion efficiencies would result. All calculations performed actually obtain the temperature excursion ΔT as a function x and t added on to the ambient level T_B. Thus, one can

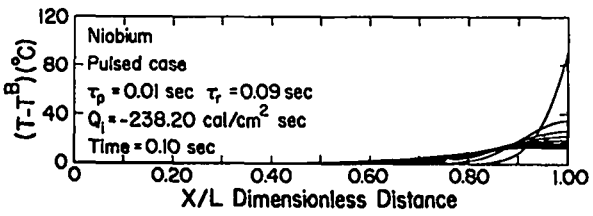

Fig. 5. Temperature profiles in a 1 cm thick Niobium wall with an incident flux of 238.2 cal/cm2 sec (1 kW/cm2). Each line represents .01 sec of elapsed time.

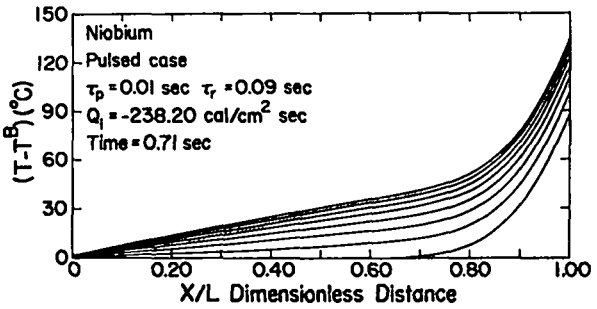

Fig. 6. Temperature profiles for Nb continued from Fig. 5. Each line drawn at the end of every pulse. (Δt = .1 sec).

obtain the actual surface temperature directly from Table III by using the appropriate T_B.

Effect of Wall Thickness

One method of circumventing the poor thermal characteristics of materials such as Al_2O_3 is to reduce the wall thickness. Ribe and associates [1] handled this problem in the θ-pinch machine by designing a composite wall consisting of 0.1 cm Al_2O_3 onto 0.3 cm of Nb. In our model, reducing the wall thickness of Al_2O_3 to 0.5 cm lowers the inside surface temperature rise to 420°C, Fig. 7, compared to 444°C for 1 cm wall with the same time and loading. The difference continues to increase until steady state is reached. Estimation of the steady state surface temperature was determined by extrapolation to $t \to \infty$ on a semilogarithmic plot of T_S versus 1/t. The y-intercept, 1/t = 0, corresponds to infinite time. Results for 1, 0.5 and 0.1 cm Al_2O_3 walls are given in Fig. 8. In each case, Q_1 was 238.2 cal/cm^2-sec ~ (1 kW/cm^2).

TABLE III

SUMMARY OF RESULTS FROM PULSED CASE

H generation = 0 $\quad h = 14$ cal/cm^2 sec °C $\quad T_B = 800$°C

$\tau_p = .01$ sec $\quad \tau_r = .09$ sec

Material	Q_i* kW/cm^2	ℓ cm	Δt micro-sec	t_f sec (last pulse)	ΔT_S at t_f °C	T_S at t_f °C	ΔT_S^{∞}‡ °C	T_S^{∞}‡ °C
Copper								
Cu	10.0	1.0	40	4.51	528	1327	529	1328
Cu	1.0	1.0	40	0.11	37	837	51	851
Alumina								
Al_2O_3	10.0	1.0	1000	1.01	3254	4054	~4200	~5000
Al_2O_3	5.0	1.0	1000	2.71	2148	2948	~2700	~3500
Al_2O_3	2.0	1.0	1000	20.61	1587	2387	1850	2650
Al_2O_3	1.0	1.0	1000	17.01	765	1565	900	1700
Al_2O_3	0.5	1.0	1000	5.01	263	1063	400	1200
Al_2O_3	0.1	1.0	1000	6.01	56	856	60	860
Al_2O_3	1.0	.5	250	3.21	421	1221	490	1290
Al_2O_3	.5	.5	250	1.61	176	976	220	1020
Al_2O_3	.1	.5	250	1.61	35	835	45	845
Al_2O_3	1.0	.1	10	1.11	200	1000	200	1000
Al_2O_3	.5	.1	10	.21	98	898	110	910
Al_2O_3	.1	.1	10	.11	19	818	25	825
Niobium								
Nb	10	1.0	200	3.31	2074	2874	2400	3200
Nb	1.0	1.0	200	2.01	188	988	220	1020
Nb	.5	1.0	200	1.41	86	886	100	900
Nb	.1	1.0	200	1.41	17	817	20	820
Nb	1.0	.5	80	1.01	140	940	150	950
Moly.								
Mo	10	1.0	90	.21	750	1550	1280	2080
Mo	1.0	1.0	90	.41	84	884	125	925
Mo	.5	1.0	90	.81	99	849	60	860
Mo	.1	1.0	90	.31	8	808	13	813

* 1 kW/cm^2 $\cong$ 238.2 cal/sec cm^2

‡ extrapolated to ∞ time

Estimated steady state surface temperatures varied from ~ 1000°C for a 0.1-cm wall to ~1290°C for a 0.5-cm wall to ~ 1700°C for a 1-cm wall with an 800°C lithium blanket.

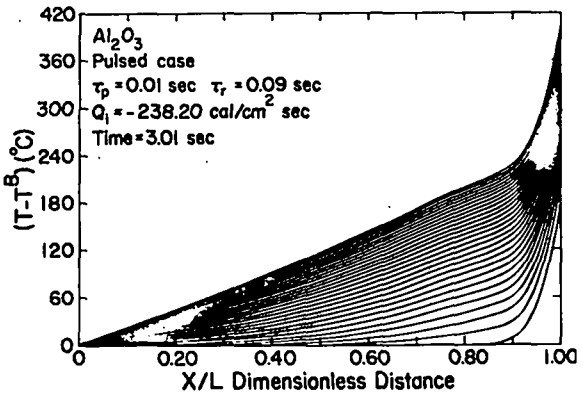

Fig. 7. Temperature profiles for a .5 cm Al203 wall with an incident flux of 238.2 cal/cm^2 sec (1 kW/cm^2). Approach to a steady state temperature distribution after 31 pulses with each line appearing at the end of every pulse. (Δt = .1 sec).

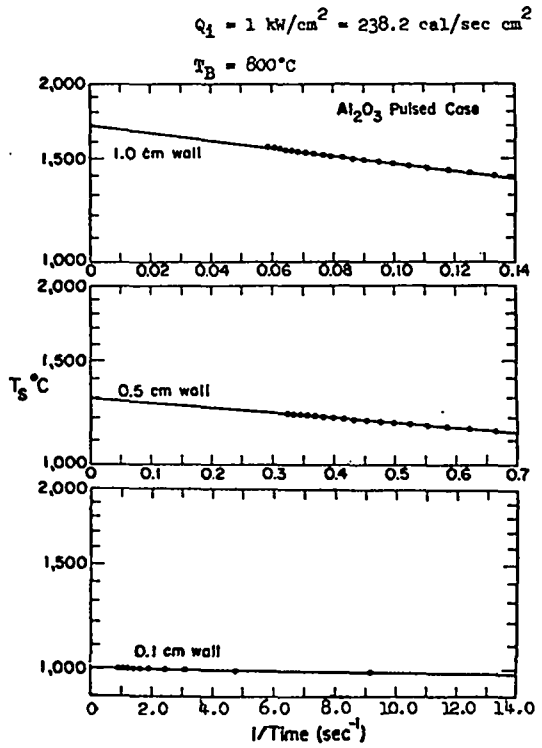

Fig. 8. Surface temperature (inside) of the first wall. Extrapolations to infinite time are shown for a 1 cm, .5 cm, and .1 cm Al_2O_3 wall with a loading of 283.2 cal/cm^2 sec (1 kW/cm^2).

Approach to Steady State

When a steady state is reached, the temperature profile will stabilize except near the inside surface where it is continuously pulsed. A one-dimensional steady state temperature profile should be linear for fixed boundary conditions. Thus, a linear profile is anticipated for a large portion of the wall not subject to the pulsing fluctuations. In Fig. 9 profiles are drawn following the first pulse, before the next eight pulses and following the ninth pulse, t = 0.81 sec. Profiles at times prior to each remaining pulse up to 3.2 sec and then following the 33rd pulse, t = 3.21 sec are shown in Fig. 10. A linear profile is found for approximately 85% of the wall distance.

If the thermal time constant of the wall τ_w, defined as

$$\tau_w = t^2/\alpha = \rho \frac{c_p t^2}{k}$$

is large compared to the rest time τ_r = .09 sec, successive pulsing will raise the ambient wall temperature above T_B since the recovery time is insufficient to allow complete relaxation. This is

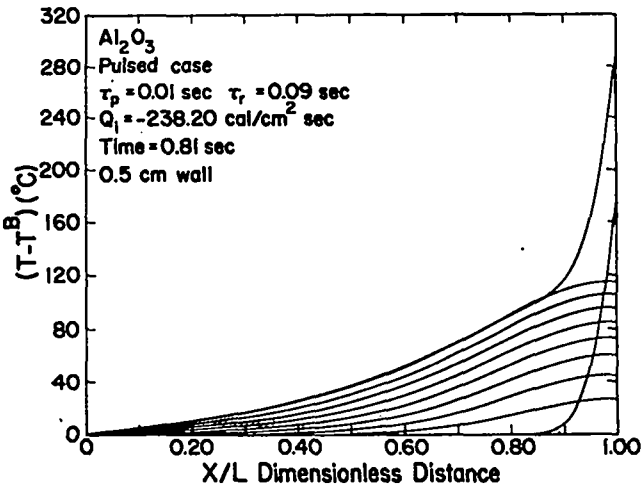

Fig. 9. Temperature profiles for a .5 cm Al_2O_3 wall with an incident flux of 238.2 cal/cm^2 sec (1 kW/cm^2)

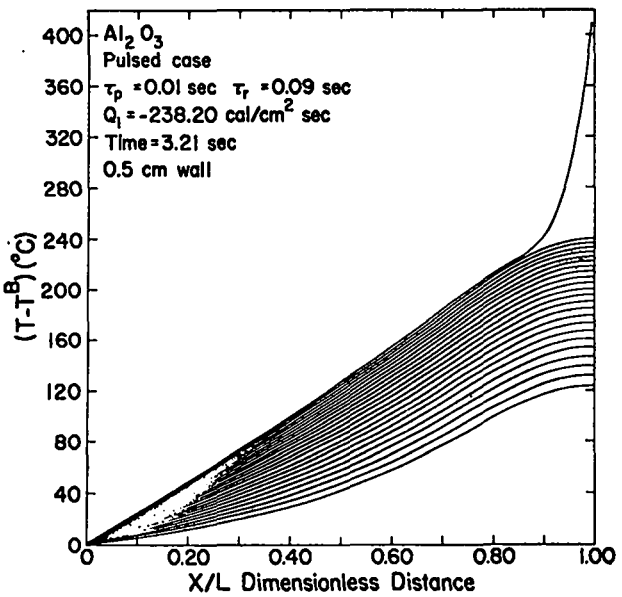

Fig. 10. Temperature profiles for a .5 cm Al_2O_3 wall with an incident flux of 238.2 cal/cm^2 sec (1 kW/cm^2).

clearly the case for a 1 cm Al_2O_3 wall, $\tau_w > 20$; however, good conductors such as copper and molybdenum have large α's and $\tau_w \lesssim \tau_r$ allowing the surface temperature T_s to more completely recover to the ambient level before the next pulse. In effect, T_s at steady state is a superposition of the ambient temperature level rise and the thermal spike due to bremsstrahlung during each pulse. Values for steady state surface temperatures, T_s^∞ and ΔT_s^∞, were extrapolated from log T_s versus 1/t plots for most of the cases listed in Table III.

Because of this superposition effect, ΔT_s^∞ can be approximated by:

$$\Delta T_s^\infty \cong \Delta T)_{\text{ambient}} + \Delta T)_{\text{1st pulse}}$$

where

$$\Delta T)_{\text{ambient}} \cong [Q_i \tau_p/(\tau_p + \tau_r)] \frac{\ell}{k}$$

$\Delta T)_{\text{1st pulse}}$ = increase in surface temperature after 1st pulse.

For example, with a 1 cm Al_2O_3 wall at 1 kW/cm^2 wall loading, ΔT_s^∞ = 900 from Table III. Calculating ΔT_s^∞ from the above equation:

$$\Delta T_s^\infty \cong \frac{(238.2)\ (.1)\ (1)}{.034} + 180 = 880°C$$

Thus, the agreement is quite good.

Liquid Metal Heat Transfer Effects

The last effect to be studied is the liquid metal heat transfer coefficient. In the results discussed so far, we purposely chose a large value of h = 14 cal/cm^2-sec-°C to maintain the outside wall at approximately 800°C. Nonetheless, in Fig. 4 one can see the effect of this large but finite h as the temperature at $x/\ell = 0$ rises above 800°C. In the case depicted in Fig. 4 a flux of 2382 cal/cm^2-sec $\approx$ (10 kW/cm^2) was maintained for 10% of the total cycle time. When steady state is achieved, ΔT at the outside surface ($x/\ell = 0$) can be approximated by $\Delta T = Q_i\ (0.1)/h \cong 17°C$ for a 0.1 duty cycle factor which agrees quite well with the numerical solution of Fig. 4.

A test was conducted on Al_2O_3 to demonstrate the effect of a low value of h. Using h = 0.14 cal/cm^2-sec-°C, a 0.5 cm wall, and a flux loading of 283.2 cal/cm^2-sec, a run was made for 25 sec (250 pulses) to approach steady state (see Fig. 11). The outside surface was heated to 972°C as compared to 805°C when h = 14 cal/cm^2-sec-°C. A realistic value of the liquid metal heat transfer coefficient should be used in any final analysis of the first wall.

Chemical Erosion and Stability

The problem of first wall reaction in a reducing environment is treated as a subset of the more general problem, viz. determination of thermodynamic properties for systems composed of many gaseous constituents in equilibrium with a pure solid phase. Complete absence of either experimental or theoretical rate data necessitate using such an idealized model.

The basis for these calculations[5] is well known having been established by Gibbs and employed previously by the Bureau of Mines[6] for power plant fuel mixtures, NASA[7] for propulsion calculations and NOTS[8] on explosion characteristics.

All calculations are made assuming an equilibrium state is reached or the equivalent assumption, that the ratio of computed to actual extent of reaction is unity. Reasonableness of this approximation

can be assessed only in the light of still to be determined experimental data.

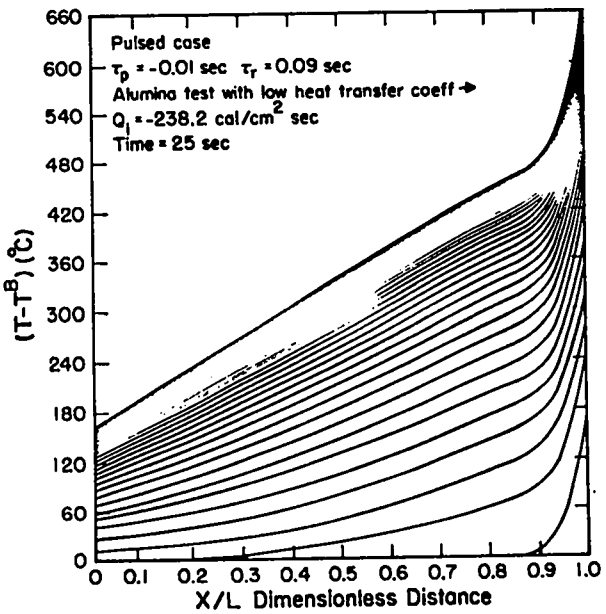

Fig. 11. Temperature profiles for a 1 cm Al_2O_3 wall with an incident wall flux of 238.2 cal/cm^2 sec (1 kW/cm^2) and a low liquid Li heat transfer coefficient h = .14 cal/cm^2 sec °C. Each line appears at the end of every pulse (Δt = .1 sec).

Because plasma cooling (heat dump), internal heat generation, and surface heat transfer coefficients were either ignored or inadequately represented in previous sections of this report, three temperatures were used in these calculations, viz. 827,1227 and 1727°C.

Uncertainty of actual fuel pressures prompted most calculations to be carried out at 1, 5, and 10 Torr, however, in Table XX the range has been extended to 1 x 10^{-5} torr as an indication of pressure effects. Finally, since the geometrical aspects of the CTR design are not finalized, gas-to-solid ratios take on the values of 0.1, 1.0, and 10. Thus, the analysis considers cases in which the number of gaseous species is one tenth the number of solid molecules, are equal or there are ten times as many gaseous species as their are solid molecules.

Briefly, the equilibrium problem consists of finding that set of n_i values which minimizes

The Gibbs free energy,

$$G = \sum_i \mu_i n_i \qquad (4)$$

subject to the side condition of a mass balance

$$\sum_i a_{i,e} n_i = Q_e \qquad (5)$$

where:

G = Gibbs free energy, cal/mole
$\mu_i = (\partial G / \partial n_i)$ at constant T and P
n_i = moles of substance i
$a_{i,e}$ = number of atoms of element e in species i
Q_e = total moles of element e

Appendix B describes the method used in this report; a method which differs from those previously mentioned[6,7,8]. The primary innovation in this work is solving a set of stiff differential equations. Gear[9] has written a code for the numerical solution of systems of ordinary differential equations which uses multistep predictor-corrector methods whose order and step-size are automatically varied consistent with specified tolerances on the estimated error. The user has the option of applying either a form of the Adams method or methods suitable for "stiff" equations; i.e., systems in which the solutions have widely different time constants. It is the latter option which makes Gear's subroutine uniquely valuable for our calculations. Thus, an experiment which took 244 iterations and ~15 to 20 sec to reach convergence in the stiff mode failed to converge in 5 min and 60,000 iterations using the Adams method.

Results of Stability Calculations

A summary of results is provided in Table IV and V. The reader must keep in mind these values were obtained on the basis of an idealized system in which the solid and gas phases are at the same temperature, i.e the assumed wall temperature, every gaseous substance acts as an ideal gas and most important, every fuel-gas solid phase collision is fruitful. The final column was computed assuming equilibrium is attained during each cycle or every gas species impinges on the wall and reacts. Little significance should be attached to the substitution of hydrogen for deuterium-tritium.

TABLE IV

Gaseous Reaction — Insulator + H_2 ⟶ Products
Pressure = 1 torr — Ratio 1 Mole H/1 Mole Insulator

Material	Temperature °C	Insulator Eroded Mole Fraction	Insulator Loss gms/year
BeO	827	1.91×10^{-10}	1.59
BeO	1227	3.84×10^{-7}	3.20×10^{3}
BeO	1727	3.00×10^{-4}	2.50×10^{6}
Al_2O_3	827	1.27×10^{-10}	4.03
Al_2O_3	1227	5.42×10^{-7}	1.72×10^{4}
Al_2O_3	1727	2.46×10^{-4}	7.80×10^{6}
BN	827	1.11×10^{-9}	8.57
BN	1227	4.71×10^{-6}	3.63×10^{4}
BN	1727	2.01×10^{-3}	1.55×10^{7}

TABLE V

Gaseous Reaction — Insulator + H ⟶ Products
Pressure = 1 torr — Ratio 1 Mole H/1 Mole Insulator

Material	Temperature °C	Insulator Eroded Mole Fraction	Insulator Loss gms/year
BeO	827	2.27×10^{-1}	1.89×10^{9}
BeO	1227	1.57×10^{-1}	1.31×10^{9}
BeO	1727	1.56×10^{-2}	1.30×10^{8}
Al_2O_3	827	8.90×10^{-2}	2.82×10^{9}
Al_2O_3	1227	3.51×10^{-2}	1.11×10^{9}
Al_2O_3	1727	2.15×10^{-2}	6.8×10^{8}
BN	827	1.67×10^{-1}	1.29×10^{9}
BN	1227	1.59×10^{-1}	1.23×10^{9}
BN	1727	1.43×10^{-1}	1.10×10^{9}
SiC	827	1.67×10^{-1}	2.46×10^{9}

Oxide Materials

Alumina

A most widely suggested inner surface material has been alumina. At equilibrium the system Al_2O_3, H_2 contains at least the additional species H, H_2O, AlH, Al, Al_2O, AlOH, AlO_2H, AlO, AlO_2, HAlO, Al_2O_2, OH, O_2, O, HO_2, H_2O_2 each at some partial pressure. Calculating the extent of reaction which one mole of Al_2O_3 solid undergoes to form the above mentioned products, one obtains at 1100°K (827°C) a value like 1×10^{-10} mole fraction. Only a trivial dependence on pressure or gas/solid ratio as Table C-1 (Appendix C) illustrates, is observed.

At 1500K (1227 C) in a H_2 environment the Al_2O_3 initially present has diminished considerably. If equilibrium is attained during every pulse-rest cycle, the computed extent of reaction from a mole of Al_2O_3 (s) translates to roughly 1000 grams per year. The major products, as shown in Table C-II, are H_2O and aluminium plus various aluminium compounds. One anticipates many of the products will be removed during the flushing process but some, such as aluminium metal, may react e.g. $NbAl_3$ is a stable material.

When the calculation is completed with the system at 2000 (1727°C), an erosion loss of roughly 10^6 grams per year is estimated. As shown in Table C-III, a reaction probability value, ϵ , of 10^{-3} to 10^{-4} would be required to prevent substantial erosion losses.

We also computed what sort of stability is expected from Al_2O_3 (s) when hydrogen atoms are included in the system. An appropriate model would employ various H/H_2 ratios with Al_2O_3, since the final H_2 and H concentrations were not available and in view of previously mentioned uncertainties, the calculation was made using a pure hydrogen atom environment. Computational-wise, this is accomplished by eliminating the recombination reaction $2H \rightleftharpoons H_2$.

The results are listed in Tables C-IV to C-VI. It is clear that regardless of temperature, pressure or gas/solid variations, hydrogen atom bombardment could have grave consequences. It would require an extremely small value for the reaction probability, ϵ , to compensate the system energetics at equilibrium.

Our model does not permit reaction between ions and Al_2O_3 (s). Any ions leaking through the magnetic barrier or produced outside it by high energy particles would be expected to react with a higher probability than the lower energy atoms.

Beryllia

A second prominently mentioned material is BeO. Its thermal conductivity is reported to be approximately thrice that of Al_2O_3. When all possible reaction products available to us are included in the H_2, BeO system at 1100 K (827°C), our model predicts BeO will be stable over the pressure range and gas/solid ratios computed. Actual product concentrations and extent of reaction with a mole of BeO are listed in Table C-VII. Increasing the temperature to 1500 K (1277°C), estimated BeO losses are sufficient to pose a potential problem, Table C-VIII. Actual loss may not correspond to the extent of reaction should a reasonable value of the reaction probability, ϵ be found.

Results given in Table C-IX were computed at 2000 K (1725°C). These data indicate BeO to be unstable over the pressures and ratios considered.

Again as in the Al_2O_3 case, if hydrogen atoms are allowed to react with a mole of BeO (s), the results in Tables C-X thru C-XII predict unacceptable consequences.

Nitride Materials

Boron Nitride

Boron nitride is a good thermal conductor, poor electrical conductor and has been used for many years by high temperature chemists. It is easily fabricated and relatively inexpensive.

The actual calculation proved to be instructional. Unlike the oxides, where only in the BeO-H_2 system was it necessary to rewrite the equations, the temperature dependence of ΔG_f° (T) for such species as BH_3, BH_2, NH_3, H and H_2 vary to an extent which makes recasting the fundamental chemical reactions mandatory for different temperatures. As an example, whereas the choice of H and BH_2 for components suffices at 2000K, convergence was not attained in five minutes at 1100K. Rewriting the chemical reactions with NH_3 and BH_3 as components, convergence was attained in fifteen seconds. Further rewriting using the gaseous component pairs BH_3, H_2 and BH_2, H_2 was necessary before the series of runs was completed.

At 1100K the loss of BN due to erosion in a molecular hydrogen atmosphere was acceptable, see Table C-XIII.

At 1500K erosion of BN under conditions of this model may be severe as shown in Table C-XIV. When a temperature of 2000K (Table C-XV) is used, predicted erosion loss is sufficient that unless an extremely favorable reaction probability were found, BN would be of little value.

As we now anticipate, should BN be exposed to hydrogen atom bombardment at any temperature of interest, predicted erosion would be most sever. The main products being BH_3, NH_3, BH_2, B_2, H_6 and $B_3N_3H_6$. All products being gaseous at 800°C and

therefore lost during flushing. Results for this system are given in Tables C-XVI thru C-XVIII.

Carbide Materials

SiC

Carbides generally are metallic like conductors. One of the exceptions is SiC, it being a semi-conductor. After the computations were finished, this material was suggested as a possible first wall material.

One run was made at 1000K in a hydrogen atom atmosphere; the results as anticipated indicate the material decomposes. (See Table C-IX).

DISCUSSION

The conditions imposed on the first wall are sufficiently in conflict that a yes-no judgement to a particular material for either the first wall or its inner surface can not be prudently made. Employing the heat flux and duty cycles suggested viz. 2382 cal/cm^2 sec $\approx$ (10kW/cm^2) and 10 percent respectively plus keeping in mind other first wall functions, none of the proposed materials look feasible. By relaxing the flux a factor of ten, ignoring the heat dump and estimating a single heat transfer coefficient, a wall thickness of about a millimeter looks possible for Al_2O_3. With these design parameters a steady state temperature of approximately 1000°C is attained with a mm of Al_2O_3. Realistically, this is a very conservative estimate. In addition to ignoring the heat dump and heat generation terms, Al_2O_3 will react with liquid lithium, necessitating a protective layer. Alumina then becomes the inner surface of the first wall and two heat transfer coefficients are required for a calculation, one between Al_2O_3 and say Nb and another between Nb and liquid lithium. Finally, it is clear that the steady state temperature is not the peak surface temperature. Results of heat transfer calculations even after flux reduction to 238.2 cal/cm^2 sec $\approx$ (1 kW/cm^2) an inner surface temperature at least two hundred degrees higher than the bulk coolant temperature, 800°C, is assured.

Stability calculations suggest a potential problem with proposed ceramic inner surfaces at these temperatures. At 800°C either Al_2O_3 or BeO would appear suitable, however, as more realistic temperatures are considered, BeO with its larger negative free energy of formation is preferred.. Table VI illustrates relative stabilities as determined by a free energy of formation criterion at 1000K. These bar graphs can be taken as a rough guide in judging oxides of greatest stability. Some materials which appear to be less stable may in actual practice be more stable with a favorable reaction probability. What our heat transfer and stability calculations suggest is a compromise. A thin wall means lower surface temperatures and a reduction in the extent of reaction. A thin wall also means reduction of mechanical strength. As the amount of material is diminished, a decrease in elapsed time before insulator replenishment is anticipated.

Atomic as well as ionic gaseous species must be excluded from contacting the inner surface. A Maxwellian distribution was assumed in the gas phase through out these calculations. During the rest period, τ_r, when a plasma dump contribution takes place we are not certain if energy attenuation is sufficient to make this assumption valid. If it is not, a greater insulator loss is anticipated.

In conclusion, BeO with its better thermal conductivity and larger negative free energy is preferred as an inner surface material within the limitations of the report.

Current Work and Speculations

The authors use this section to present their thoughts concerning problems these calculations raise. Clearly, what is needed is an easily fabricated, good thermal but poor electrical conducting material with a high free energy of formation. In addition, it should be inert to liquid lithium or if not adhere to a material that does.

All of the proposed ceramic materials are poor thermal conductiors, therefore, we speculate on means to enhance their heat transfer characteristics.

Consider an oxide solid solution such as $ZrO_2Y_2O_3$. Individually both are poor thermal conductors. In solution, however, substitutional vacancies appear proportional to the amount of Y_2O_3 added. Presumably, such defects are introduced symmetrically without distrubing the original lattice wave component of the thermal conductivity.

The possibility of an additional conduction mode due to such vacancies has yet to be ruled out. If no improvement is found with the introduction of ordered vacancies, their remains a possibility

of enhancement by trapping gas molecules, e.g. Helium in the vacancies. Such trapped molecules provide another possible mechanism for heat conduction by using the intermolecular contacts between trapped gas and matrix to transfer energy. This behavior would be analogous to that observed with clathrate compounds.[10]

Some laboratory work along these lines is in progress. A series of ZrO_2 samples doped with CaO and Y_2O_3 are now being investigated to determine the effect of vacancies and temperature on the thermal properties of ZrO_2. Two samples ZrO_2 (2 CaO) and ZrO_2 ($.2Y_2O_3$) were subjected to 3.5 mev aphas at .5 μ amp for 1 and 5 hours respectively. The calcia doped sample showed a loss in thermal diffusivity and an increase in volume, whereas ytteria doped material indicated a slight enhancement of diffusivity and no change in volume.

If the thermal properties of the first wall cannot be improved by either altering physical or chemical properties, then a radial composite such as suggested earlier[11] or a "slinky" design[4] could be investigated. Al_2O_3 is known to adhere to Nb (2% Zr) by formation of $NbAl_3$, similarity ZrO_2 can be made to adhere to Nb (2% Zr) by forming a seal with $ZrPt_3$. In either case, a two-dimensional relaxation technique incorporating many of the features of the present code could be used to analyze heat transfer requirements.

Finally, the possibility of oxidation in place can be considered. The free energy of formation of ZrO_2 is similar to Al_2O_3, that of Y_2O_3 slightly lower, like BeO, see Table VI. One anticipates reaction products would be mainly metal and water. Because these metals have high heats of vaporization viz 98 kcal/mole for Y and 146 kcal/mole for Zr, they would not leave during flushing and could be reoxidized in situ. This possibility is greatly diminished with light element oxides e.g. Be, Al, Mg, Ca or Si. Similar reasoning holds for BN and SiC.

For NbO the free energy of formation at 1000K is 45 keal less than that of BeO, (see Table VI) and is probably a poor thermoconductor. If the flushing operation could be carried out with a H_2/H_2O mixture, a very thin NbO film would be produced on a niobium metal first wall. Its dielectric strength would have to be investigated and its stability in a reducing environment would certainly be poorer than the materials thus far considered; nevertheless, with frequent reoxidation it might be satisfactory. Further investigation along these lines using vanadium as a first wall material may also prove interesting, $\Delta G^f_{vo} \approx 101$ kcal/mole.

It seems mandatory to determine the relation between the computed extent of reaction and the actual extent of reaction or the reaction probability by laboratory experiments. Some work in this field by Rosner and associates is illuminating. His experiments are confined to work on polycrystalline refractory metals such as W, Mo and Ta and their reaction probabilities with F/F_2, O/O_2 and other feed gases. Experimentally, values for the reaction probability, ϵ, range from 10^{-6} to 0.8. These values vary with temperature, pressure and atom to molecule ratios.

CONCLUSIONS.

1. A numerical program for analyzing heat transfer effects at the first wall, with the capability of using time, temperature, or position dependent properties, various boundary conditions or internal heat generation terms in obtaining temperature profiles has been implemented.

2. Steady state temperature profiles were established for Cu, Al_2O_3, and Nb with various wall loadings (.1 to 10 kW/cm^2) and thicknesses. (1 to 1.0 cm)

3. An idealized model was constructed and a program implemented capable of ascertaining the extent of reaction accompanying plasma-fuel, first-wall material interactions.

4. Chemical erosion losses were determined for Al_2O_3, BeO, and BN as functions of temperature, pressure and gas/solid ratios, and a criteria was suggested to minimize erosion losses.

5. A method of fabrication as a means of providing the required in situ dielectric properties was suggested.

RECOMMENDATIONS.

1. A more realistic range of design variables should be established. These should include (a) a clearer definition of total energy deposition (bremsstralung, neutron, etc.) fluxes as a function of depth into the wall, and (b) specification of the heat loads for the plasma cooling part of the cycle.

2. The feasibility of enhancing the thermal properties of a poor conductor by altering

TABLE VI

RELATIVE OXIDE STABILITY

$XM(s) + \frac{1}{2} O_2(g) = MxO(s)$

ΔG°_{1000} (bar graph is a relative scale)

Li_2O -110	BeO -120	B_2O_3 -82	C											N	O	F
Na_2O -66	MgO -118	Al_2O_3 -108	SiO_2 -83											P	S	Cl
K_2O -50	CaO -126	Sc_2O_3 -112	TiO -91	VO -79	Cr_2O_3 -70	MnO -74	FeO -48	CoO -39	NiO -35	Cu_2O -25	ZnO -59	Ga_2O -59	GeO -42	As_2O_3 -34	SeO_2 -12	Br
Rb_2O -44	SrO -118	Y_2O_3 -116	ZrO_2 -108	NbO -70	MoO_2 -49	Tc	RuO -8	RhO -12	Pd	Ag	CdO -38	In_2O_3 -48	SnO -45	Sb_2O_3 -35	TeO_2 -17	I
Cs_2O -38	BaO -111	La_2O_3 -119	HfO_2 -110	Ta_2O_5 -77	WO_2 -48	Re -32	Os	Ir	Pt	Au	Hg	Tl_2O_3 -27	PbO -29	Bi_2O_3 -24	Po	At
Fr	RaO -106	Ac_2O_3 -128														

Ce_2O_3 -119	Pr_2O_3 -125	Nd_2O_3 -118	Pm	Sm_2O_3 -122	Eu	Gd	Tb	Dy	Ho	Er	Tm	Yb	Lu
ThO_2 -123	Pa	UO_2 -109	NpO_2 -102	PuO_2 -102	Am	Cm	Bk	Cf	Es	Fm	Md	No	Lw

its lattice structure should be thoroughly investigated.

3. In anticipation of a possible need for composite materials, a two-dimensional relaxation procedure should be incorporated into the current code for estimating temperature profiles.

4. Reaction probabilities must be determined for any seriously proposed insulator.

5. A computer model which would estimate (a) the ratio of molecular to atomic species striking the wall and (b) the velocity distribution of the gaseous species is desirable.

6. If no insulator material is exposed to the gas phase, then the effect of sputtering on the metal surface should be investigated.

ACKNOWLEDGEMENTS

The authors are indebted to the people in C-7 especially M. Wells, R. Bivins, R. C. Blandford and M. Stein. We wish, also, to thank J. Phillips of P-14 for his encouragement.

REFERENCES

1. Ianniello, L. C., (ed.), "Fusion Reactor First Wall Materials," AEC Conference, Germantown, Maryland, Jan. 27-28, 1972 (April, 1972).

2. "Proceedings of the Int. Working Sessions on Fusion Reactor Technology," June 28-July 2, 1971, Oak Ridge National Laboratory, CONF-710624 (1971).

3. Burnett, S. C., W. R. Ellis, T. A. Ohphant, and F. L. Ribe, "The Reference Theta Pinch Reactor (RTPR), A Study of a Pulsed High Beta Fusion Reactor Based on the Theta Pinch," Internal report (Aug. 1972).

4. Phillips, J. A., private communication (Aug. 1972).

5. Zeleznik, F. J., and S. Gordon, NASA, TN D-473 (1960).

6. Brinkley, S. R., "High Speed Aerodynamics and Jet Propulsion - Combustion Processes, Vol. II, 64-98, Princeton University Press (1956).

7. Zeleznik, F. J., and S. Gordon, NASA, TN D-1454 (1962).

8. Villars, D. S., Proc. 1st Conf. High Temp. Systems, 141-51 (1960).

9. Gear, C. W., Commun. ACM 14, 176 (1971).

10. Tester, J. W., C. C. Herrick, and R. L. Bivins, "The Use of Monte Carlo in Calculating the Thermodynamic Properties of Water Clathrates," A.I. Ch.E.J. 18, 1220 (1972).

11. Memo to J. Phillips, May 1971 from C. C. Herrick.

APPENDIX A

DIFFERENTIAL EQUATION SPECIFICATIONS

Numerical Method for Initial Value Problems

Equation to be solved:

$$\alpha \frac{\partial^2 T}{\partial x^2} = \frac{\partial T}{\partial t} + \frac{C}{k} \qquad \text{(A-1)}$$

Approximations for a wall divided into m divisions at the nth time interval

$$\frac{\partial T_{m,n}}{\partial t} = \frac{T_{m,n+1} - T_{m,n}}{\Delta t} \qquad \text{(A-2)}$$

$$\left(\frac{\partial^2 T_{m,n}}{\partial x^2}\right) = \frac{T_{m+1,n} - 2T_{m,n} + T_{m-1,n}}{\Delta x^2} \qquad \text{(A-3)}$$

Solving for $T_{m,\, n+1}$ using Eqs. (A-1), (A-2) and (A-3),

$$T_{m,n+1} = MT_{m+1,\, n} + (1 - 2M)\, T_{m,\, n} + MT_{m-1,\, n} + \frac{C}{k} \Delta t \qquad \text{(A-4)}$$

where:

$$M = \frac{\alpha \Delta t}{\Delta x^2} \qquad \text{(A-5)}$$

This will converge to a stable solution of $M \leq \frac{1}{2}$. Thus, one has to be careful in choosing Δx and Δt to keep $M \leq \frac{1}{2}$.

The boundary conditions were implimented as follows:

(1) At $x = 0$ (outside wall) liquid metal heat transfer

$$-k \left(\frac{\partial T}{\partial x}\right)_{x=0} = h \left(T - T_B\right)_{x=0} \qquad \text{(A-6)}$$

$$\frac{T_{1,\, n} - T_{0,\, n}}{\Delta x} = \frac{-h}{k} \left(T_{0,\, n} - T_B\right) \qquad \text{(A-7)}$$

(2) At $x = \ell$ (inside wall) incident flux

$$-k \left(\frac{\partial T}{\partial x}\right)_{x=\ell} = Q_i \qquad \text{(A-8)}$$

$$\frac{T_{m,\, n} - T_{m-1,\, n}}{\Delta x} = \frac{-Q_i}{k} \qquad \text{(A-9)}$$

An initial temperature of 800°C = T_B was chosen for all x, and Eq. (A-4) with boundary conditions (A-7) and (A-9) was used to perform the iteration

APPENDIX B

CHEMICAL STABILITY ANALYSIS

Principle of Method

For a system of m elements and s chemical species the number of components c is equal to the rank $C \leq m$ of the matrix of the stoichiometric coefficients a_{ie}. Here a_{ie} is the number of atoms of element e present in the chemical substance i. Any component c is represented by a linearly independent formula vector α_c:

$$\alpha_c = (a_{c1}, \ldots a_{ce} \ldots a_m) \qquad \text{(B-1)}$$

There are (s-c) substances hereafter designated j whose formula vectors α_j are dependent vectors, expressable as linear combinations of the independent vectors α_c,

$$\alpha_j = \sum_c \nu_{jc} \alpha_c \qquad \text{(B-2)}$$

These (s-c), substances j are defined as species since they are obtained from Eq. (B-2). The choice of c components is arbitrary. Eq. (B-2) corresponds to reactions between components A_c to form a Species A_j:

$$\sum_c \nu_{jc} A_c = A_j \qquad \text{(B-3)}$$

As usual, ν_{jc} are the stoichiometric coefficients of the j^{th} reaction which produces a given species A_j.

Any particular reaction j will proceed to an extent γ corresponding to the final equilibrium state. In this final equilibrium state, the system will contain $\sum_c \nu_{jc} (1 - \gamma)$ moles of component c and γ moles of the j species. For a given temperature and pressure, the Gibbs free energy of this system is $G = \sum_i \mu_i n_i$ or

$$G = \sum_c \nu_{jc} (1 - \gamma) \mu_c + \gamma \mu_j \qquad \text{(B-4)}$$

The equilibrium state by definition is the state of minimum G i.e. $(\partial G / \partial \gamma) = 0$.
With this condition Eq. (B-4) becomes

$$\sum_c \nu_{jc} \mu_c = \mu_j \qquad \text{(B-5)}$$

For an ideal gas

$$\mu_i = \mu^\circ_i + RT \ln p_i$$

so Eq. (B-5) becomes

$$\sum_c \nu_{jc} (\mu^\circ_j + RT \ln p_c) = \mu^\circ_j + RT \ln p_j$$

or

$$RT \ln \frac{p_j}{\prod_c (p_c)^{\nu_{jc}}} = -(\mu^\circ_j - \sum_c \nu_{jc} \mu^\circ_c) \qquad \text{(B-6)}$$

The term on the right hand side is the standard Gibbs free energy of the j^{th} reaction and is hereafter designated $(\Delta G^\circ)^j_{Rx}$

Consequently, Eq. (B-6) is written as:

$$M \frac{p_j}{\prod_c (Pc)} \nu_{jc} = -\frac{(\Delta G^\circ)^j_{Rx}}{RT} = \ln (K_{pj})_{Rx} \qquad \text{(B-7)}$$

Tabulated values of $(\Delta G^\circ)^j_{Rx}$ such as the JANAF compilation are used to compute values of K_{pj}. In our treatment all gaseous substances are assumed to be ideal i.e.

$$p_i = x_i p_{total} = \frac{n_i}{\sum_i n_i} p_{total}$$

whereupon for any species n_j e.g.(B-7) takes the form

$$n_j = K_{pj} \left(\frac{p_{total}}{\sum_i n_i}\right)^{(\sum_c \nu_{jc} - 1)} \prod_c n_c^{\nu_{jc}} \qquad \text{(B-8)}$$

It is clear that we have as many equations of this type as we have gaseous species i.e. (s - c). It is only necessary then to obtain $C \leq m$ more equations to completely define the system.

An obvious constraint on the system is that of constant mass. The number of moles of any specific element is not a variable but subject to the constraint

$$\delta n_{total} = 0 \qquad \text{(B-9)}$$

A set of n_c values which form the solution must satisfy the mass balance conditions.

$$\sum_s A_{se} n_s = Q_e \qquad \text{(B-10)}$$

Here A_{se} is the number of atoms of element e present in any substance i and Q_e is a system constant. By writing a mass balance equation for each component of the system, the requiste number of equations and unknowns are obtained.

The working expressions are Eq's, (B-8), (B-10) and a summation over n_{ie}, the total number of moles of gas at equilibrium:

$$n = n_1 + n_2 + \ldots + n_s = \sum_c^s n_{ie}.$$

With numerical values substituted for the equilibrium constants, K_{pj} (T), the masses, Q_e, and the pressure, p_{total}, these working equations are of the form

$$f_j = f_i (n_1, \ldots n_s)_j \quad i = 1, \ldots, s \qquad \text{(B-11)}$$

for a given i the solution of

$$f_i (n_1 \ldots\ldots, \ldots n_s) = 0 \qquad \text{(B-12)}$$

yields only certain values if Eq. (B-12) holds. Any arbitary set of n_i will yield a value of $f_i \neq 0$. This permits us to define an error

$$\epsilon_i = \epsilon_i (n_1 \ldots, \ldots n_s) \qquad \text{(B-13)}$$

which is clearly zero for the unique set of n_i corresponding to Eq. (B-12). For present purposes, the method of steepest decent was chosen to obtain values for the n's. This procedure determines the set of values for $n_1 \ldots n_s$ such that

$$S = \sum_{i=1}^{s} \epsilon_i^2 \qquad \text{(B-14)}$$

has a local minimum.

By involving a search parameter λ the error functions can be used to calculate differentials of the form

$$\frac{dm_j}{d\lambda} = -\sum_{i=1}^{s} \epsilon_i \frac{\partial \epsilon_i}{\partial n_j} \; ; \; j = 1, \ldots s$$

The Gear method of handling stiff equations computes values for derivatives of S viz;

$$\frac{dS}{d\lambda} = -2 \sum_{j=1}^{s} \left(\frac{dn_j}{d\lambda}\right)^2$$

until value the sum of squares in Eq. (B-14) becomes less than 10^{-20}.

The square root of this value, 10^{-10} moles, keeps the computation time from becoming excessive and corresponds roughly to an extent of reaction of one gram per year for the problem at hand.

Illustration of the Method

A. Define every chemical species that may be important to the system under investigation.

B. Determine the rank of the formula matrix if the number of components is not intuitively obvious. Table B-I presents the matrix for the BN-H_2 system.

C. Select the components and write a series of chemical reactions each involving one species and components, see Table B-II.

D. Compute the Gibbs free energy of formation and/or equilibrium constant for each reaction. Results in Table B-II came from the JANAF tables.

E. Write as many mass balance equations as there are components.

F. Transform the mass balance and mass action equations into error functions.

G. Differentiate the error functions with respect to every concentration variable and sum.

TABLE B-I

MATRIX FOR THE BN-H_2 SYSTEM

			B	H	N
j	C	BN(s)	1	0	1
	1	BH_3	1	3	0
	2	NH_3	0	3	1
3		BN	1	0	1
4		H	0	1	0
5		NH	0	1	1
6		NH_2	0	2	1
7		N_2H_2	0	2	2
8		N_2	0	0	2
9		N_2H_4	0	4	2
10		B	1	0	0
11		BH	1	1	0
12		BH_2	1	2	0
13		B_2	2	0	0
14		B_2H_6	2	6	0
15		B_5H_9	5	9	0
16		$B_{10}H_{14}$	10	14	0
17		H_2	0	2	0
18		$B_3N_3H_6$	3	6	3

TABLE B-II

CHEMICAL REACTION FOR BN-H_2SYSTEM

	$(\Delta G°)_{Rx}$ 1100K
$BH_3 + NH_3 = 6H + BN(s)$	142.781
$2NH_3 + BN(s) = 3NH + BH_3$	288.319
$5NH_3 + BN(s) = 6NH_2 + BH_3$	279.055
$4NH_3 + BN(s) = 3N_2H_2 + 2BH_3$	307.934
$NH_3 + BN(s) = N_2 + BH_3$	51.231
$5NH_3 + BN(s) = 3N_2H_4 + BH_3$	226.888
$NH_3 + BN(s) = 2B(g) + BH_3$	209.427
$2BH_3 + BN(s) = 3BH + NH_3$	229.375
$5BH_3 + BN(s) = 6BH_2 + NH_3$	119.665
$BH_3 + BN(s) = B_3(g) + NH_3$	167.694
$2BH_3 = B_2H_6$	-4.056
$4BH_3 + BN(s) = B_5H_9 + NH_3$	43.074
$22BH_3 + 8BN(s) = 3B_{10}H_{14} + 8NH_3$	292.433
$BN(s) = BN(g)$	121.878
$BH_3 + NH_3 = 3H_2 + BN$	-86.419
$2BN + NH_3 + BH_3 = B_3N_3H_6$	15.274

T = 1100 AL_2O_3 (1 mole) + H_2 (.5 mole) COMPONENTS ARE H_2 AND H_2O

Table C-I

Pressure $H_2(g)/Al_2O_3(s)$	1.			5.			10.		
SPECIES (Mole fract)	.1	1.	10.	.1	1.	10.	.1	1.	10.
H	7.09×10^{-7}	7.09×10^{-7}	7.09×10^{-7}	3.17×10^{-7}	3.17×10^{-7}	3.17×10^{-7}	2.24×10^{-7}	2.24×10^{-7}	2.24×10^{-7}
H_2O	8.24×10^{-9}	1.11×10^{-9}	4.85×10^{-10}	9.71×10^{-9}	1.03×10^{-9}	2.98×10^{-10}	9.37×10^{-9}	1.01×10^{-9}	2.49×10^{-10}
ALH	5.87×10^{-10}	$<10^{-10}$	$<10^{-10}$	6.91×10^{-10}	$<10^{-10}$	$<10^{-10}$	6.67×10^{-10}	$<10^{-10}$	$<10^{-10}$
AL	5.07×10^{-10}	1.19×10^{-10}	2.10×10^{-10}	5.95×10^{-10}	*	*	5.74×10^{-10}	*	*
Al_2O	6.72×10^{-10}	$<10^{-10}$	$<10^{-10}$	7.92×10^{-10}	*	*	7.65×10^{-10}	*	*
AlOH	2.51×10^{-10}	*	*	2.95×10^{-10}	*	*	2.85×10^{-10}	*	*
AlO_2H	$<10^{-10}$	*	*	$<10^{-10}$	*	*	$<10^{-10}$	*	*
AlO	1.68×10^{-10}	*	*	1.98×10^{-10}	*	*	1.91×10^{-10}	*	*
AlO_2	$<10^{-10}$	*	*	$<10^{-10}$	*	*	$<10^{-10}$	*	*
Al_2O_2	3.36×10^{-10}	*	*	3.96×10^{-10}	*	*	3.82×10^{-10}	*	*
OH	$<10^{-10}$	*	*	$<10^{-10}$	*	*	$<10^{-10}$	*	*
O_2	*	*	*	*	*	*	*	*	*
O	*	*	*	*	*	*	*	*	*
HO_2	*	*	*	*	*	*	*	*	*
H_2O_2	*	*	*	*	*	*	*	*	*
H	9.99×10^{-1}	9.99×10^{-1}	9.99×10^{-1}	9.99×10^{-1}	9.99×10^{-1}	9.99×10^{-1}	9.99×10^{-1}	9.99×10^{-1}	9.99×10^{-1}
HALO	2.50×10^{-10}	$<10^{-10}$	$<10^{-10}$	2.95×10^{-10}	$<10^{-10}$	$<10^{-10}$	2.85×10^{-10}	$<10^{-10}$	$<10^{-10}$
(MOLES GAS)Total	5.0×10^{-2}	.5000	5.00	5.00×10^{-2}	.5000	5.00	5.00×10^{-2}	5.00×10^{-2}	5.000
MOLES Al_2O_3 REMAINING	1.000000	1.0000	1.0000	1.000000	1.0000	1.0000	1.0000	1.0000	1.0000
MOLES Al_2O_3 ERODED	8.8×10^{-11}	1.27×10^{-10}	7.72×10^{-10}	1.04×10^{-10}	1.12×10^{-10}	4.59×10^{-10}	1.002×10^{-10}	1.10×10^{-10}	3.73×10^{-10}

T = 1500K

Al_2O_3 (1 mole) + H_2 (.5 mole) COMPONENTS ARE H_2 AND H_2O

Table C-II

Pressure $H_2(g)/Al_2O_3$	1.			5.			10.		
SPECIES (Mole fract)	.1	1.	10.	.1	1.	10.	.1	1.	10.
H	4.83×10^{-4}	4.83×10^{-4}	4.83×10^{-4}	2.16×10^{-4}	2.16×10^{-4}	2.16×10^{-4}	1.53×10^{-4}	1.53×10^{-4}	1.53×10^{-4}
H_2O	3.16×10^{-6}	3.16×10^{-6}	3.16×10^{-6}	1.70×10^{-6}	1.69×10^{-6}	1.69×10^{-6}	1.30×10^{-6}	1.30×10^{-6}	1.30×10^{-6}
AlH	6.99×10^{-8}	6.93×10^{-8}	6.93×10^{-8}	7.95×10^{-8}	7.90×10^{-8}	7.90×10^{-8}	8.34×10^{-8}	8.30×10^{-8}	8.30×10^{-8}
Al	1.96×10^{-6}	1.97×10^{-6}	1.97×10^{-6}	1.00×10^{-6}	1.00×10^{-6}	1.00×10^{-6}	7.44×10^{-7}	7.46×10^{-7}	7.47×10^{-7}
Al_2O	3.76×10^{-8}	3.69×10^{-8}	3.68×10^{-8}	2.64×10^{-8}	2.57×10^{-8}	2.57×10^{-8}	2.24×10^{-8}	2.18×10^{-8}	2.18×10^{-8}
AlOH	5.48×10^{-8}	5.45×10^{-8}	5.44×10^{-8}	3.36×10^{-8}	3.33×10^{-8}	3.38×10^{-8}	2.72×10^{-8}	2.69×10^{-8}	2.68×10^{-8}
AlO_2H	$< 10^{-10}$	$< 10^{-10}$	$< 10^{-10}$	$< 10^{-10}$	$< 10^{-10}$	$< 10^{-10}$	$< 10^{-10}$	$< 10^{-10}$	$< 10^{-10}$
AlO	2.23×10^{-10}	2.88×10^{-11}	*	2.16×10^{-10}	*	*	2.07×10^{-10}	*	*
AlO_2	$< 10^{-10}$	$< 10^{-10}$	*	$< 10^{-10}$	*	*	$< 10^{-10}$	*	*
Al_2O_2	4.32×10^{-10}	*	*	4.29×10^{-10}	*	*	4.12×10^{-10}	*	*
OH	$< 10^{-10}$	*	*	$< 10^{-10}$	*	*	$< 10^{-10}$	*	*
O_2	*	*	*	*	*	*	*	*	*
O	*	*	*	*	*	*	*	*	*
HO_2	*	*	*	*	*	*	*	*	*
H_2O_2	*	*	*	*	*	*	*	*	*
H_2	9.995×10^{-1}	9.995×10^{-1}	9.995×10^{-1}	9.998×10^{-1}	.9998	.9998	9.998×10^{-1}	9.998×10^{-1}	9.998×10^{-1}
HAlO	4.10×10^{-10}	$< 10^{-10}$	$< 10^{-10}$	4.14×10^{-10}	$< 10^{-10}$	$< 10^{-10}$	4.02×10^{-10}	$< 10^{-10}$	$< 10^{-10}$
(MOLES GAS)Total	5.00×10^{-2}	.5001	5.0012	$5.\times10^{-2}$	.50005	5.0005	5.0×10^{-2}	.50004	5.0004
MOLES Al_2O_3 REMAINING	.9999	.9999	.9995	.99999	.99999	.99999	.9999	.9999	.9999
MOLES Al_2O_3 ERODED	5.42×10^{-8}	5.42×10^{-7}	5.42×10^{-6}	2.92×10^{-8}	2.92×10^{-7}	2.92×10^{-6}	2.25×10^{-8}	2.25×10^{-7}	2.25×10^{-6}

T = 2000

Al_2O_3 (1 mole) + H_2 (.5 mole) COMPONENTS ARE H_2 AND H_2O

Table C-III

Pressure (torr) $H_2(g)/Al_2O_3(s)$ SPECIES (Mole fract)	1.			5.			10.		
	.1	1.	10.	.1	1.	10.	.1	1.	10.
H	4.36×10^{-2}	4.36×10^{-2}	4.36×10^{-2}	1.98×10^{-2}	1.98×10^{-2}	1.98×10^{-2}	1.40×10^{-2}	1.40×10^{-2}	1.40×10^{-2}
H_2O	1.33×10^{-3}	1.33×10^{-3}	1.33×10^{-3}	7.21×10^{-4}	7.21×10^{-4}	7.21×10^{-4}	5.54×10^{-4}	5.54×10^{-4}	5.54×10^{-4}
AlH	7.01×10^{-6}	7.01×10^{-6}	7.01×10^{-6}	8.24×10^{-6}	8.24×10^{-6}	8.24×10^{-6}	8.75×10^{-6}	8.75×10^{-6}	8.75×10^{-6}
Al	7.88×10^{-4}	7.88×10^{-4}	7.88×10^{-4}	4.09×10^{-4}	4.09×10^{-4}	4.09×10^{-4}	3.06×10^{-4}	3.06×10^{-4}	3.06×10^{-4}
Al_2O	5.76×10^{-5}	5.76×10^{-5}	5.76×10^{-5}	4.10×10^{-5}	4.10×10^{-5}	4.10×10^{-5}	3.52×10^{-5}	3.52×10^{-5}	3.52×10^{-5}
AlOH	4.84×10^{-5}	4.84×10^{-5}	4.84×10^{-5}	3.01×10^{-5}	3.01×10^{-5}	3.01×10^{-5}	2.44×10^{-5}	2.44×10^{-5}	2.44×10^{-5}
AlO_2H	3.27×10^{-7}	3.27×10^{-7}	3.27×10^{-7}	1.08×10^{-7}	1.08×10^{-7}	1.08×10^{-7}	6.68×10^{-8}	6.68×10^{-8}	6.68×10^{-8}
AlO	1.47×10^{-6}	1.47×10^{-6}	1.47×10^{-6}	4.05×10^{-7}	4.05×10^{-7}	4.05×10^{-7}	2.32×10^{-7}	2.32×10^{-7}	2.32×10^{-7}
AlO_2	1.11×10^{-9}	1.28×10^{-9}	1.30×10^{-9}	$< 10^{-10}$	1.70×10^{-10}	1.88×10^{-10}	$< 10^{-10}$	$< 10^{-10}$	$< 10^{-10}$
Al_2O_2	3.90×10^{-9}	3.55×10^{-9}	3.51×10^{-9}	1.69×10^{-9}	1.37×10^{-9}	1.33×10^{-9}	1.23×10^{-9}	9.10×10^{-10}	8.72×10^{-10}
OH	6.02×10^{-6}	6.02×10^{-6}	6.02×10^{-6}	1.45×10^{-6}	1.45×10^{-6}	1.45×10^{-6}	7.83×10^{-7}	7.83×10^{-7}	7.83×10^{-7}
O_2	$< 10^{-10}$	$< 10^{-10}$	1.13×10^{-10}	$< 10^{-10}$	$< 10^{-10}$	$< 10^{-10}$	$< 10^{-10}$	$< 10^{-10}$	$< 10^{-10}$
O	2.02×10^{-7}	2.02×10^{-7}	2.02×10^{-7}	2.10×10^{-8}	2.14×10^{-8}	2.14×10^{-8}	7.81×10^{-9}	8.13×10^{-9}	8.17×10^{-9}
HO_2	$< 10^{-10}$	$< 10^{-10}$	$< 10^{-10}$	$< 10^{-10}$	$< 10^{-10}$	$< 10^{-10}$	$< 10^{-10}$	$< 10^{-10}$	$< 10^{-10}$
H_2O_2	*	*	*	*	*	*	*	*	*
H_2	9.54×10^{-1}	9.54×10^{-1}	9.54×10^{-1}	9.79×10^{-1}	9.79×10^{-1}	9.79×10^{-1}	9.85×10^{-1}	9.85×10^{-1}	9.85×10^{-1}
HAlO	6.16×10^{-10}	2.75×10^{-10}	2.39×10^{-10}	5.05×10^{-10}	1.87×10^{-10}	1.50×10^{-10}	4.81×10^{-10}	1.61×10^{-10}	1.23×10^{-10}
(MOLES GAS) Total	5.12×10^{-2}	5.12×10^{-1}	.5116	5.05×10^{-2}	.5052	5.0523	5.12×10^{-1}	.5037	5.0371
MOLES Al_2O_3 REMAINING	.99998	.99975	.9975	.99998	.99987	.9987	.9998	.9999	.9989
MOLES Al_2O_3 ERODED	2.46×10^{-5}	2.46×10^{-4}	2.46×10^{-3}	1.34×10^{-5}	1.34×10^{-4}	1.34×10^{-4}	2.46×10^{-4}	1.03×10^{-4}	1.03×10^{-3}

T = 1100K

AL_2O_3 + H COMPONENTS ARE H AND H_2O

Mole Fraction

Table C-IV

Pressure Ratio H(g)/Al_2O_3(s) SPECIES	1 Torr			5 Torr			10 Torr		
	.1	1.	10.	.1	1.	10.	.1	1.	10.
H	3.926×10^{-1}	3.92×10^{-1}	3.92×10^{-1}	2.458×10^{-1}	2.458×10^{-1}	2.458×10^{-1}	1.971×10^{-1}	1.97×10^{-1}	1.97×10^{-1}
H_2O	3.644×10^{-1}	3.64×10^{-1}	3.64×10^{-1}	4.525×10^{-1}	4.525×10^{-1}	4.525×10^{-1}	4.817×10^{-1}	4.82×10^{-1}	4.82×10^{-1}
ALH	2.429×10^{-1}	2.43×10^{-1}	2.43×10^{-1}	3.017×10^{-1}	3.017×10^{-1}	3.017×10^{-1}	3.211×10^{-1}	3.21×10^{-1}	3.21×10^{-1}
AL	1.670×10^{-6}	1.70×10^{-6}	1.70×10^{-6}	6.740×10^{-7}	6.740×10^{-7}	6.739×10^{-7}	4.471×10^{-7}	4.47×10^{-7}	4.47×10^{-7}
Al_2O	6.556×10^{-8}	6.51×10^{-8}	6.51×10^{-8}	3.251×10^{-8}	3.236×10^{-8}	3.243×10^{-8}	2.328×10^{-8}	2.36×10^{-8}	2.37×10^{-8}
AlOH	2.153×10^{-5}	2.15×10^{-5}	2.15×10^{-5}	1.694×10^{-5}	1.694×10^{-5}	1.694×10^{-5}	1.493×10^{-5}	1.49×10^{-5}	1.49×10^{-5}
AlO_2H	$<10^{-10}$	$<10^{-10}$	$<10^{-10}$	4.700×10^{-10}	$<10^{-10}$	$<10^{-10}$	3.111×10^{-10}	$<10^{-10}$	$<10^{-10}$
AlO	1.241×10^{-10}	$<10^{-10}$	$<10^{-10}$	$<10^{-10}$	$<10^{-10}$	$<10^{-10}$	$<10^{-10}$	$<10^{-10}$	$<10^{-10}$
AlO_2	$<10^{-10}$	*	*	*	*	*	*	*	*
Al_2O_2	2.482×10^{-10}	*	*	*	*	*	*	*	*
OH	$<10^{-10}$	*	*	4.479×10^{-10}	*	*	4.054×10^{-10}	*	*
O_2	*	*	*	$<10^{-10}$	*	*	3.768×10^{-10}	*	*
O	*	*	*	*	*	*	1.884×10^{-10}	*	*
HO_2	*	*	*	4.037×10^{-10}	*	*	5.938×10^{-10}	*	*
H_2O_2	*	*	*	8.958×10^{-10}	*	*	8.107×10^{-10}	*	*
HALO	*	*	*	5.141×10^{-10}	*	*	1.227×10^{-10}	*	*
(MOLES) Total	7.329×10^{-2}	.73290	7.3290	6.885×10^{-2}	.6885x10	6.8846	.067488	.67488	6.7488
MOLES Al_2O_3 AFTER REACTION	.9911	.910963	.10963	.98961	.89615	-3.849×10^{-2}	.989162	.89162	-8.374×10^{-2}
MOLES Al_2O_3 ERODED	8.904×10^{-3}	.089037	.89037	.010385	.10385	1.03849	.010837	.10837	1.08375

T = 1500K

Al_2O_3 + H COMPONENTS ARE H AND H_2O

Table C-V

Pressure Ratio H(g)/Al_2O_3 SPECIES(Mole fract)	Mole Fraction 1.			5.			10.		
	.1	1.	10.	.1	1.	10.	.1	1.	10.
H	8.05×10^{-1}	8.05×10^{-1}	8.05×10^{-1}	6.45×10^{-1}	6.45×10^{-1}	6.45×10^{-1}	5.65×10^{-1}	5.65×10^{-1}	5.65×10^{-1}
H_2O	1.16×10^{-1}	1.16×10^{-1}	1.16×10^{-1}	2.13×10^{-1}	2.13×10^{-1}	2.13×10^{-1}	2.61×10^{-1}	2.61×10^{-1}	2.61×10^{-1}
ALH	7.58×10^{-2}	7.58×10^{-2}	7.58×10^{-2}	1.41×10^{-1}	1.41×10^{-1}	1.41×10^{-1}	1.73×10^{-1}	1.73×10^{-1}	1.73×10^{-1}
AL	1.29×10^{-3}	1.29×10^{-3}	1.29×10^{-3}	6.00×10^{-4}	6.00×10^{-4}	6.00×10^{-4}	4.21×10^{-4}	4.21×10^{-4}	4.21×10^{-4}
Al_2O	2.10×10^{-4}	2.10×10^{-4}	2.10×10^{-4}	1.29×10^{-4}	1.29×10^{-4}	1.29×10^{-4}	1.01×10^{-4}	1.01×10^{-4}	1.01×10^{-4}
AlOH	7.89×10^{-4}	7.89×10^{-4}	7.89×10^{-4}	8.36×10^{-4}	8.36×10^{-4}	8.36×10^{-4}	8.20×10^{-4}	8.20×10^{-4}	8.20×10^{-4}
AlO_2H	5.08×10^{-10}	2.63×10^{-10}	2.54×10^{-10}	$<10^{-10}$	1.21×10^{-10}	1.54×10^{-10}	$<10^{-10}$	1.02×10^{-10}	1.24×10^{-10}
AlO	$<10^{-10}$	$<10^{-10}$	$<10^{-10}$	$<10^{-10}$	$<10^{-10}$	$<10^{-10}$	$<10^{-10}$	$<10^{-10}$	$<10^{-10}$
AlO_2	$<10^{-10}$	$<10^{-10}$	$<10^{-10}$	1.25×10^{-10}	$<10^{-10}$	$<10^{-10}$	$<10^{-10}$	$<10^{-10}$	$<10^{-10}$
Al_2O_2	$<10^{-10}$	$<10^{-10}$	$<10^{-10}$	$<10^{-10}$	$<10^{-10}$	$<10^{-10}$	$<10^{-10}$	$<10^{-10}$	$<10^{-10}$
OH	1.26×10^{-9}	9.72×10^{-10}	9.53×10^{-10}	3.75×10^{-10}	3.97×10^{-10}	4.34×10^{-10}	$<10^{-10}$	2.75×10^{-10}	3.07×10^{-10}
O_2	2.19×10^{-10}	$<10^{-10}$	$<10^{-10}$	5.01×10^{-10}	$<10^{-10}$	$<10^{-10}$	2.94×10^{-10}	$<10^{-10}$	$<10^{-10}$
O	1.10×10^{-10}	$<10^{-10}$	$<10^{-10}$	2.50×10^{-10}	$<10^{-10}$	$<10^{-10}$	1.47×10^{-10}	$<10^{-10}$	$<10^{-10}$
HO_2	4.17×10^{-10}	$<10^{-10}$	$<10^{-10}$	1.91×10^{-10}	$<10^{-10}$	$<10^{-10}$	$<10^{-10}$	$<10^{-10}$	$<10^{-10}$
H_2O_2	6.16×10^{-10}	$<10^{-10}$	$<10^{-10}$	$<10^{-10}$	$<10^{-10}$	$<10^{-10}$	$<10^{-10}$	$<10^{-10}$	$<10^{-10}$
HALO	1.87×10^{-10}	$<10^{-10}$	$<10^{-10}$	$<10^{-10}$	$<10^{-10}$	$<10^{-10}$	$<10^{-10}$	$<10^{-10}$	$<10^{-10}$
(MOLES) Total	.08961	.896914	8.9691	.082503	.82503	8.2503	.079351	.79351	7.9351
MOLES Al_2O_3 AFTER REACTION	.996489	.96489	.64890	.99412	.94121	.41209	.99308	.93078	.30787
MOLES Al_2O_3 ERODED	3.51×10^{-3}	.03511	.35110	5.879×10^{-3}	.058790	.5879	6.921×10^{-3}	.069213	.69213

T = 2000K

AL_2O_3 (1 mole) + H (1 mole) COMPONENTS ARE H and H_2O

Table C-VI

Pressure (torr)	1.			5.			10.		
H(g)/Al_2O_3	.1	1.	10.	.1	1.	10.	.1	1.	10.
Species(Mole fract.)									
H	9.04×10^{-1}	9.04×10^{-1}	9.04×10^{-1}	8.52×10^{-1}	8.52×10^{-1}	8.52×10^{-1}	8.16×10^{-1}	8.16×10^{-1}	8.16×10^{-1}
H_2O	5.72×10^{-2}	5.72×10^{-2}	5.72×10^{-2}	8.87×10^{-2}	8.87×10^{-2}	8.87×10^{-2}	1.10×10^{-1}	1.10×10^{-1}	1.10×10^{-1}
AlH	4.58×10^{-3}	4.58×10^{-3}	4.58×10^{-3}	2.09×10^{-2}	2.09×10^{-2}	2.09×10^{-2}	3.60×10^{-2}	3.60×10^{-2}	3.60×10^{-2}
Al	2.48×10^{-2}	2.48×10^{-2}	2.48×10^{-2}	2.40×10^{-2}	2.40×10^{-2}	2.40×10^{-2}	2.16×10^{-2}	2.16×10^{-2}	2.16×10^{-2}
Al_2O	5.73×10^{-3}	5.73×10^{-3}	5.73×10^{-3}	9.38×10^{-3}	9.38×10^{-3}	9.38×10^{-3}	1.03×10^{-2}	1.03×10^{-2}	1.03×10^{-2}
AlOH	3.17×10^{-3}	3.17×10^{-3}	3.17×10^{-3}	5.05×10^{-3}	5.05×10^{-3}	5.05×10^{-3}	5.88×10^{-3}	5.88×10^{-3}	5.88×10^{-3}
AlO_2H	2.15×10^{-6}	2.15×10^{-6}	2.15×10^{-6}	1.20×10^{-6}	1.20×10^{-6}	1.20×10^{-6}	9.42×10^{-7}	9.42×10^{-7}	9.42×10^{-7}
AlO	4.66×10^{-6}	4.66×10^{-6}	4.66×10^{-6}	1.57×10^{-6}	1.57×10^{-6}	1.57×10^{-6}	9.58×10^{-7}	9.58×10^{-7}	9.58×10^{-7}
AlO_2	3.77×10^{-10}	4.07×10^{-10}	4.13×10^{-10}	$<10^{-10}$	$<10^{-10}$	$<10^{-10}$	$<10^{-10}$	$<10^{-10}$	$<10^{-10}$
Al_2O_2	3.51×10^{-8}	3.50×10^{-8}	3.50×10^{-8}	2.02×10^{-8}	2.00×10^{-8}	2.00×10^{-8}	1.48×10^{-8}	1.48×10^{-8}	1.48×10^{-8}
OH	1.25×10^{-5}	1.25×10^{-5}	1.25×10^{-5}	4.12×10^{-6}	4.12×10^{-6}	4.12×10^{-6}	2.67×10^{-6}	2.67×10^{-6}	2.67×10^{-6}
O_2	$<10^{-10}$	$<10^{-10}$	$<10^{-10}$	$<10^{-10}$	$<10^{-10}$	$<10^{-10}$	$<10^{-10}$	$<10^{-10}$	$<10^{-10}$
O	2.02×10^{-8}	2.02×10^{-8}	2.02×10^{-8}	1.24×10^{-9}	1.42×10^{-9}	1.42×10^{-9}	5.07×10^{-10}	4.93×10^{-10}	4.81×10^{10}
HO_2	$<10^{-10}$	$<10^{-10}$	$<10^{-10}$	$<10^{-10}$	$<10^{-10}$	$<10^{-10}$	3.46×10^{-10}	$<10^{-10}$	$<10^{-10}$
H_2O_2	$<10^{-10}$	$<10^{-10}$	$<10^{-10}$	$<10^{-10}$	$<10^{-10}$	$<10^{-10}$	6.34×10^{-10}	$<10^{-10}$	$<10^{-10}$
HAlO	1.52×10^{-8}	1.54×10^{-8}	1.54×10^{-8}	2.46×10^{-8}	2.45×10^{-8}	2.45×10^{-8}	2.88×10^{-8}	2.86×10^{-8}	2.86×10^{-8}
(MOLES GAS)Total	.09476	.97408	9.7408	.09476	.94763	9.4763	.09275	.92756	9.2756
MOLES Al_2O_3 REMAINING	.99674	.97853	.78532	..99674	.96742	.67421	.99610	.96099	.60988
MOLES Al_2O_3 ERODED	3.26×10^{-3}	.021468	.21468	3.26×10^{-3}	.03258	.32578	3.90×10^{-3}	3.90×10^{-2}	.39012

T + 1100 K- BeO (1 mole) + H_2 (.5 mole) COMPONENTS ARE H_2O AND H

Table C-VII

Pressure(torr)	1.			5.			10.		
H/BeO	.1 ‡	1.	10.	.1 ‡	1. ‡	10.	.1 ‡	1. ‡	10.
SPECIES in mole fract									
H	7.09×10^{-7}	7.09×10^{-7}	7.09×10^{-7}	3.17×10^{-7}	3.17×10^{-7}	3.17×10^{-7}	2.24×10^{-7}	2.24×10^{-7}	2.24×10^{-7}
H_2O	4.45×10^{-9}	7.28×10^{-10}	2.47×10^{-10}	3.99×10^{-9}	4.84×10^{-10}	2.44×10^{-10}	4.20×10^{-9}	4.91×10^{-10}	2.43×10^{-10}
BeH	*	*	*	*	*	*	*	*	*
BeOH	*	*	*	*	*	*	*	*	*
BeH_2	*	*	*	*	*	*	*	1.93×10^{-10}	1.85×10^{-10}
$Be(OH)_2$	*	*	*	*	*	*	*	*	*
Be_2O	*	*	*	*	*	*	*	*	*
H_2	9.99×10^{-1}	9.99×10^{-1}	9.99×10^{-1}	9.99×10^{-1}	9.99×10^{-1}	9.99×10^{-1}	9.99×10^{-1}	9.99×10^{-1}	9.99×10^{-1}
OH	*	*	*	*	*	*	*	*	*
Be	*	*	*	*	*	*	*	*	*
O_2	*	*	*	*	*	*	*	*	*
BeO	*	*	*	*	*	*	*	*	*
Be_2O_2	*	*	*	*	*	*	*	*	*
Be_3O_3	*	*	*	*	*	*	*	*	*
Be_4O_4	*	*	*	*	*	*	*	*	*
Be_5O_5	*	*	*	*	*	*	*	*	*
Be_6O_6	*	*	*	*	*	*	*	*	*
O	*	*	*	*	*	*	*	*	*
TOTAL MOLES OF GAS	.0500	.5000	5.000	.0500	.5000	5.000	.0500	.5000	5.000
MOLES BeO LEFT	1.000	1.000	1.000	1.000	1.000	1.000	1.000	1.000	1.000
MOLES BeO ERODED	1.94×10^{-10}	1.91×10^{-10}	1.08×10^{-9}	1.74×10^{-10}	2.26×10^{-10}	1.07×10^{-9}	1.84×10^{-10}	2.29×10^{-10}	1.07×10^{-9}

* Moles less than 10^{-10}
‡ Components are H_2 and H_2O

T = 1500K

BeO (1 Mole) + H_2 (.5 Mole) COMPONENTS H_2O AND H

Table C-VIII

Pressure (torr)	1.			5.			10.		
H/BeO	.1	1.	10.	.1	1.	10.	.1	1.	10.
SPECIES in Mole fraction									
H	4.83×10^{-4}	4.83×10^{-4}	4.83×10^{-4}	2.61×10^{-4}	2.16×10^{-4}	2.16×10^{-4}	1.53×10^{-4}	1.53×10^{-4}	1.53×10^{-4}
H_2O	7.70×10^{-7}	7.67×10^{-7}	7.67×10^{-7}	3.83×10^{-7}	3.81×10^{-7}	3.81×10^{-7}	3.01×10^{-7}	2.99×10^{-7}	2.99×10^{-7}
BeH	2.20×10^{-9}	1.48×10^{-9}	1.41×10^{-9}	*	1.35×10^{-9}	1.28×10^{-9}	*	1.27×10^{-9}	1.15×10^{-9}
BeOH	1.08×10^{-9}	*	8.07×10^{-10}	*	3.88×10^{-10}	3.63×10^{-10}	*	2.86×10^{-10}	2.58×10^{-10}
BeH_2	4.48×10^{-8}	4.40×10^{-8}	4.39×10^{-8}	8.89×10^{-8}	8.86×10^{-8}	8.86×10^{-8}	1.13×10^{-7}	1.13×10^{-7}	1.13×10^{-7}
$Be(OH)_2$	*	*	2.25×10^{-11}	1.09×10^{-10}	*	*	*	*	*
Be_2O	*	*	4.50×10^{-11}	4.73×10^{-10}	*	*	4.71×10^{-10}	*	*
H_2	9.99×10^{-1}	9.99×10^{-1}	9.99×10^{-1}	9.99×10^{-1}	9.99×10^{-1}	9.99×10^{-1}	9.99×10^{-1}	9.99×10^{-1}	9.99×10^{-1}
OH	*	*	*	*	*	*	*	*	*
Be	7.19×10^{-7}	7.22×10^{-7}	7.23×10^{-7}	2.89×10^{-7}	2.91×10^{-7}	2.91×10^{-7}	1.84×10^{-7}	1.85×10^{-7}	1.85×10^{-7}
O_2	*	*	*	*	*	*	*	*	*
BeO(g)	*	*	*	*	*	*	*	*	*
Be_2O_2	*	*	*	*	*	*	*	*	*
Be_3O_3(g)	*	*	*	*	*	*	*	*	*
Be_4O_4(g)	*	*	*	*	*	*	*	*	*
Be_5O_5(g)	*	*	*	*	*	*	*	*	*
Be_6O_6(g)	*	*	*	*	*	*	*	*	*
O	*	*	*	*	*	*	*	*	*
TOTAL MOLES of GAS	.05001	.5001	5.001	.0500	.5000	5.000	.0500	.5000	5.000
MOLES BeO LEFT	.9999	.9999	.9999	.9999	.9999	.9999	.9999	.9999	.9999
MOLES BeO ERODED	3.84×10^{-8}	3.84×10^{-7}	3.84×10^{-6}	1.91×10^{-8}	1.91×10^{-7}	1.91×10^{-6}	1.50×10^{-8}	1.50×10^{-7}	1.50×10^{-7}

*Mole fraction less than 10^{-10}

T = 2000 K

BeO (1 mole) + H_2 (.5 mole) COMPONENTS H_2O AND H

Table C-IX

Pressure (torr)	1.			5.			10.		
H/BeO	.1	1.	10.	.1	1.	10.	.1	1.	10.
SPECIES in Mole fraction									
H	4.36×10^{-2}	4.36×10^{-2}	4.36×10^{-2}	1.97×10^{-2}	1.97×10^{-2}	1.97×10^{-2}	1.40×10^{-2}	1.40×10^{-2}	1.40×10^{-2}
H_2O	5.70×10^{-4}	5.70×10^{-4}	5.70×10^{-4}	2.59×10^{-4}	2.59×10^{-4}	2.59×10^{-4}	1.84×10^{-4}	1.84×10^{-4}	1.84×10^{-4}
BeH	8.92×10^{-7}	8.92×10^{-7}	8.92×10^{-7}	9.10×10^{-7}	9.11×10^{-7}	9.11×10^{-7}	9.14×10^{-7}	9.14×10^{-7}	9.14×10^{-7}
BeOH	1.03×10^{-5}	1.03×10^{-5}	1.03×10^{-5}	4.69×10^{-6}	4.68×10^{-6}	4.68×10^{-6}	3.32×10^{-6}	3.32×10^{-6}	3.32×10^{-6}
BeH_2	5.25×10^{-7}	5.26×10^{-7}	5.26×10^{-7}	1.21×10^{-6}	1.21×10^{-6}	1.22×10^{-6}	1.73×10^{-6}	1.73×10^{-6}	1.73×10^{-6}
$Be(OH)_2$	6.75×10^{-7}	6.75×10^{-7}	6.75×10^{-7}	3.07×10^{-7}	3.07×10^{-7}	3.07×10^{-7}	2.19×10^{-7}	2.19×10^{-7}	2.18×10^{-7}
Be_2O	1.51×10^{-6}	1.51×10^{-6}	1.51×10^{-6}	6.83×10^{-7}	6.83×10^{-7}	6.83×10^{-7}	4.83×10^{-7}	4.83×10^{-7}	4.83×10^{-7}
H_2	9.55×10^{-1}	9.55×10^{-1}	9.55×10^{-1}	9.80×10^{-1}	9.80×10^{-1}	9.80×10^{-1}	9.86×10^{-1}	9.86×10^{-1}	9.86×10^{-1}
OH	2.59×10^{-6}	2.59×10^{-6}	2.59×10^{-6}	5.20×10^{-7}	5.20×10^{-7}	5.19×10^{-7}	2.61×10^{-7}	2.61×10^{-7}	2.61×10^{-7}
Be	5.71×10^{-4}	5.71×10^{-4}	5.71×10^{-4}	2.57×10^{-4}	2.57×10^{-4}	2.57×10^{-4}	1.82×10^{-4}	1.82×10^{-4}	1.82×10^{-4}
O_2	*	*	3.12×10^{-11}	*	*	*	*	*	*
BeO(g)	5.82×10^{-8}	5.82×10^{-8}	5.82×10^{-8}	1.16×10^{-8}	1.16×10^{-8}	1.16×10^{-8}	5.82×10^{-9}	5.82×10^{-9}	5.82×10^{-9}
$Be_2O_2(g)$	3.02×10^{-8}	3.02×10^{-8}	3.02×10^{-8}	6.04×10^{-9}	6.04×10^{-9}	6.04×10^{-9}	3.02×10^{-9}	3.02×10^{-9}	3.02×10^{-9}
$Be_3O_3(g)$	2.53×10^{-7}	2.53×10^{-7}	2.53×10^{-7}	5.06×10^{-8}	5.06×10^{-8}	5.06×10^{-8}	2.53×10^{-8}	2.53×10^{-8}	2.53×10^{-8}
$Be_4O_4(g)$	2.39×10^{-8}	2.39×10^{-8}	2.39×10^{-8}	4.78×10^{-9}	4.78×10^{-9}	4.78×10^{-9}	2.39×10^{-9}	2.39×10^{-9}	2.39×10^{-9}
$Be_5O_5(g)$	*	2.00×10^{-10}	*	*	*	*	*	*	2.00×10^{-11}
$Be_6O_6(g)$	*	*	*	*	*	*	*	*	*
O	8.71×10^{-8}	8.68×10^{-8}	8.67×10^{-8}	8.15×10^{-9}	7.64×10^{-9}	7.69×10^{-9}	2.31×10^{-9}	2.67×10^{-9}	2.72×10^{-9}
TOTAL MOLES of GAS	.05114	.5114	5.114	.0505	.5051	5.051	.05036	.5036	5.036
MOLES BeO REMAINING	.9999	.9997	.9970	.9999	.9998	.9986	.9999	.9999	.9990
MOLES BeO ERODED	3.00×10^{-5}	3.00×10^{-4}	3.00×10^{-3}	1.34×10^{-5}	1.34×10^{-6}	1.34×10^{-3}	9.53×10^{-6}	9.53×10^{-5}	9.53×10^{-4}

*less than 10^{-10} moles

T = 1100K

BeO (1 Mole) + H (1 Mole) COMPONENTS ARE H AND $H_2O(g)$

Table C-X

Pressure (torr)	1.			5.			10.		
H/BeO	.1	1.	10.	.1	1.	10..	.1	1.	10.
SPECIES in Mole fraction									
H	3.41×10^{-2}	3.41×10^{-2}	3.41×10^{-2}	1.54×10^{-2}	1.54×10^{-2}	1.54×10^{-2}	1.09×10^{-2}	1.09×10^{-2}	1.09×10^{-2}
H_2O	4.83×10^{-1}	4.83×10^{-1}	4.83×10^{-1}	4.92×10^{-1}	4.92×10^{-1}	4.92×10^{-1}	4.94×10^{-1}	4.94×10^{-1}	4.94×10^{-1}
BeH	*	1.55×10^{-9}	1.55×10^{-9}	*	5.03×10^{-10}	4.53×10^{-10}	*	3.73×10^{-10}	3.23×10^{-10}
BeOH	*	*	*	*	*	*	*	*	*
BeH_2	4.83×10^{-1}	4.83×10^{-1}	4.83×10^{-1}	4.92×10^{-1}	4.92×10^{-1}	4.92×10^{-1}	4.94×10^{-1}	4.94×10^{-1}	4.94×10^{-1}
$Be(OH)_2$	6.38×10^{-8}	6.38×10^{-8}	6.38×10^{-8}	6.50×10^{-8}	6.56×10^{-8}	6.57×10^{-8}	6.53×10^{-8}	6.59×10^{-8}	6.60×10^{-8}
Be_2O	*	5.92×10^{-10}	5.92×10^{-10}	*	*	*	*	*	*
OH	*	*	*	*	*	*	*	*	*
Be	*	6.00×10^{-10}	6.00×10^{-10}	6.00×10^{-10}	*	*	5.98×10^{-10}	*	*
O_2	*	*	*	*	*	*	*	*	*
BeO	*	*	*	*	*	*	*	*	*
Be_2O_2	*	*	*	*	*	*	*	*	*
Be_3O_3	*	*	*	*	*	*	*	*	*
Be_4O_4	*	*	*	*	*	*	*	*	*
Be_5O_5	*	*	*	*	*	*	*	*	*
Be_6O_6	*	*	*	*	*	*	*	*	*
O	*	*	*	*	*	*	*	*	*
TOTAL GAS MOLES	.0509	.5468	5.468	.0504	.5039	5.039	.0503	.5027	5.027
MOLES BeO LEFT	.9754	.7734	None	.9752	.7519	None	.9751	.7514	-1.486
MO									
MOLES BeO ERODED	.0246	.2266	2.266	.0248	.2480	2.480	.0248	.2486	2.486

*Moles less than 10^{-10}

T = 1500 K

BeO (1Mole) + H (1Mole) COMPONENTS ARE H AND H_2O (g)

Table C-XI

Pressure (torr)	1.			5.			10.		
H/BeO	.1	1.	10.	.1	1.	10.	.1	1.	10.
SPECIES in Mole fraction									
H	5.40×10^{-1}	5.40×10^{-1}	5.40×10^{-1}	2.98×10^{-1}	2.98×10^{-1}	2.98×10^{-1}	2.22×10^{-1}	2.22×10^{-1}	2.22×10^{-1}
H_2O	2.30×10^{-1}	2.30×10^{-1}	2.30×10^{-1}	3.51×10^{-1}	3.51×10^{-1}	3.51×10^{-1}	3.89×10^{-1}	3.89×10^{-1}	3.88×10^{-1}
BeH	6.58×10^{-6}	6.58×10^{-6}	6.58×10^{-6}	3.64×10^{-6}	3.64×10^{-6}	3.64×10^{-6}	2.71×10^{-6}	2.71×10^{-6}	2.71×10^{-6}
BeOH	8.99×10^{-7}	8.99×10^{-7}	8.99×10^{-7}	4.97×10^{-7}	4.97×10^{-7}	4.97×10^{-7}	3.70×10^{-7}	3.70×10^{-7}	3.70×10^{-7}
BeH_2	2.30×10^{-1}	2.30×10^{-1}	2.30×10^{-1}	3.51×10^{-1}	3.51×10^{-1}	3.51×10^{-1}	3.89×10^{-1}	3.89×10^{-1}	3.89×10^{-1}
$Be(OH)_2$	6.88×10^{-6}	6.88×10^{-6}	6.88×10^{-6}	1.05×10^{-5}	1.05×10^{-5}	1.05×10^{-5}	1.16×10^{-5}	1.16×10^{-5}	1.16×10^{-5}
Be_2O	5.34×10^{-10}	2.09×10^{-10}	1.69×10^{-10}	*	*	3.79×10^{-11}	*	*	2.18×10^{-11}
OH	2.41×10^{-9}	2.76×10^{-9}	2.80×10^{-9}	1.04×10^{-9}	*	1.54×10^{-9}	*	1.10×10^{-9}	1.15×10^{-9}
Be	3.02×10^{-6}	3.02×10^{-6}	3.02×10^{-6}	6.04×10^{-7}	6.03×10^{-7}	6.03×10^{-7}	3.02×10^{-7}	3.02×10^{-7}	3.01×10^{-7}
O_2	*	*	*	*	*	*	*	*	*
BeO	*	*	*	*	*	*	*	*	*
Be_2O_2	*	*	*	*	*	*	*	*	*
Be_3O_3	*	*	*	*	*	*	*	*	*
Be_4O_4	*	*	*	*	*	*	*	*	*
Be_5O_5	*	*	*	*	*	*	*	*	*
Be_6O_6	*	*	*	*	*	*	*	*	*
O	*	*	*	*	*	*	*	*	*
TOTAL GAS MOLES	.0685	.6851	6.851	.0588	.5877	5.877	.0562	.5625	5.625
MOLES BeO LEFT	.9842	.8426	-.5745	.9794	.7937	-1.061	.9781	.7812	-1.187
MOLES BeO ERODED	.0157	.1574	1.574	.0206	.2061	2.061	.0219	.2187	2.187

*Moles less than 10^{-10}

T = 2000

BeO (1 Mole) + H (1 Mole) COMPONENTS ARE H(g) AND H_2O(g)

Table C-XII

Pressure (torr)	1.			5.			10.		
H/BeO	.1	1.	10.	.1	1.	10.	.1	1.	10.
SPECIES(Mole Fract)									
H	9.69×10^{-1}	9.69×10^{-1}	9.69×10^{-1}	9.18×10^{-1}	9.18×10^{-1}	9.19×10^{-1}	8.62×10^{-1}	8.62×10^{-1}	8.62×10^{-1}
H_2O	1.54×10^{-2}	1.54×10^{-2}	1.54×10^{-2}	4.05×10^{-2}	4.05×10^{-2}	4.05×10^{-2}	6.88×10^{-2}	6.88×10^{-2}	6.89×10^{-2}
BeH	3.60×10^{-4}	3.60×10^{-4}	3.60×10^{-4}	5.86×10^{-4}	5.86×10^{-4}	5.86×10^{-4}	5.70×10^{-4}	5.70×10^{-4}	5.70×10^{-4}
BeOH	2.30×10^{-4}	2.30×10^{-4}	2.30×10^{-4}	2.18×10^{-4}	2.18×10^{-4}	2.18×10^{-4}	2.04×10^{-4}	2.04×10^{-4}	2.04×10^{-4}
BeH_2	4.72×10^{-3}	4.71×10^{-3}	4.71×10^{-3}	3.64×10^{-2}	3.64×10^{-2}	3.64×10^{-2}	6.64×10^{-2}	6.64×10^{-2}	6.64×10^{-2}
$Be(OH)_2$	1.83×10^{-5}	1.83×10^{-5}	1.83×10^{-5}	4.80×10^{-5}	4.80×10^{-5}	4.80×10^{-5}	8.15×10^{-5}	8.15×10^{-5}	8.14×10^{-5}
Be_2O	2.76×10^{-5}	2.76×10^{-5}	2.76×10^{-5}	9.46×10^{-6}	9.46×10^{-6}	9.46×10^{-6}	4.90×10^{-6}	4.90×10^{-6}	4.90×10^{-6}
OH	3.16×10^{-6}	3.16×10^{-6}	3.16×10^{-6}	1.75×10^{-6}	1.75×10^{-6}	1.75×10^{-6}	1.58×10^{-6}	1.58×10^{-6}	1.58×10^{-6}
Be	1.04×10^{-2}	1.04×10^{-2}	1.04×10^{-2}	3.56×10^{-3}	3.56×10^{-3}	3.56×10^{-3}	1.85×10^{-3}	1.85×10^{-3}	1.85×10^{-3}
O_2	*	*	*	*	*	*	*	*	*
BeO(g)	5.82×10^{-8}	5.82×10^{-8}	5.82×10^{-8}	1.16×10^{-8}	1.16×10^{-8}	1.16×10^{-8}	5.82×10^{-9}	5.82×10^{-9}	5.82×10^{-9}
Be_2O_2	3.02×10^{-8}	3.02×10^{-8}	3.02×10^{-8}	6.04×10^{-9}	6.04×10^{-9}	6.04×10^{-9}	3.02×10^{-9}	3.02×10^{-9}	3.02×10^{-9}
Be_3O_3	2.53×10^{-7}	2.53×10^{-7}	2.53×10^{-7}	5.06×10^{-8}	5.06×10^{-8}	5.06×10^{-8}	2.53×10^{-8}	2.53×10^{-8}	2.53×10^{-8}
Be_4O_4	2.39×10^{-8}	2.39×10^{-8}	2.39×10^{-8}	4.78×10^{-9}	4.78×10^{-9}	4.78×10^{-9}	2.39×10^{-9}	2.39×10^{-9}	2.39×10^{-9}
Be_5O_5	*	2.00×10^{-10}	2.00×10^{-10}	*	*	4.00×10^{-11}	*	*	2.00×10^{-11}
Be_6O_6	*	*	*	*	*	*	*	*	*
O	4.58×10^{-9}	4.75×10^{-9}	4.76×10^{-9}	*	5.59×10^{-10}	5.56×10^{-10}	*	*	2.65×10^{-10}
(MOLES GAS)Total	9.903×10^{-2}	.9903	9.903	9.316×10^{-2}	.9316	9.316	8.82×10^{-2}	.8822	8.822
MOLES BeO REMAINING	.9984	.9844	.8439	.9962	.9620	.6197	.9939	.9390	.3899
MOLES BeO ERODED	1.56×10^{-3}	1.56×10^{-2}	.1560	3.80×10^{-3}	3.80×10^{-2}	.3803	6.10×10^{-3}	6.10×10^{-2}	.6101

*Moles less than 10^{-10}

T = 1100K

BN (1 Mole) + H_2 (1 Mole) COMPONENTS ARE H_2 and BH_2

Table C-XIII

Pressure (torr)	1.			5.			10.		
H/BN	.1	1.	10.	.1	1.	10.	.1	1.	10.
SPECIES in Mole fraction									
H_2	9.99×10^{-1}	9.99×10^{-1}	9.99×10^{-1}	9.99×10^{-1}	9.99×10^{-1}	9.99×10^{-1}	9.99×10^{-1}	9.99×10^{-1}	9.99×10^{-1}
BH_2	1.10×10^{-8}	1.69×10^{-9}	1.40×10^{-9}	8.42×10^{-9}	9.86×10^{-10}	7.35×10^{-10}	6.99×10^{-9}	7.90×10^{-10}	5.85×10^{-10}
N_2	*	7.75×10^{-10}	1.10×10^{-9}	*	4.74×10^{-10}	7.95×10^{-10}	4.51×10^{-10}	3.79×10^{-10}	6.31×10^{-10}
NH	*	*	*	*	*	*	*	*	*
NH_2	*	*	*	*	*	*	*	*	*
N_2H_2	*	*	*	*	*	*	*	*	*
NH_3	*	*	*	*	*	6.37×10^{-11}	*	*	1.12×10^{-10}
N_2H_4	*	*	*	*	*	*	*	*	*
BH_3	5.16×10^{-9}	8.08×10^{-10}	6.56×10^{-10}	8.83×10^{-9}	1.05×10^{-9}	7.70×10^{-10}	1.04×10^{-8}	1.19×10^{-9}	*
B(g)	*	*	*	*	*	*	*	*	*
BH	*	*	*	*	*	*	*	*	1.14×10^{-10}
B_2(g)	*	*	*	*	*	*	*	*	*
B_2H_6	*	*	*	*	*	*	*	*	*
B_5H_9	*	*	*	*	*	*	*	*	*
$B_{10}H_{14}$	*	*	*	*	*	*	*	*	*
$B_3N_3H_6$	*	*	*	*	*	*	*	*	*
BN(g)	*	*	*	*	*	*	*	*	*
H	7.09×10^{-7}	7.09×10^{-7}	7.09×10^{-7}	3.17×10^{-7}	3.17×10^{-7}	3.17×10^{-7}	2.24×10^{-7}	2.24×10^{-7}	2.95×10^{-9}
TOTAL GAS MOLES	.0500	.5000	5.000	.0500	.5000	5.000	.0500	.5000	5.000
MOLES BN LEFT	1.000	1.000	.9999	1.000	1.000	.9999	1.000	1.000	.9999
MOLES BN ERODED	2.79×10^{-10}	1.11×10^{-9}	1.12×10^{-8}	3.00×10^{-10}	8.09×10^{-10}	8.49×10^{-9}	2.93×10^{-10}	7.17×10^{-10}	7.25×10^{-9}

*Moles less than 10^{-10}

T = 1500

BN (1 Mole) + H_2 (1 Mole) COMPONENTS ARE H_2 AND BH_2

Table C-XIV

Pressure (torr)	1.			5.			10.		
H/BN	.1	1.	10.	.1	1.	10.	.1	1.	10.
SPECIES in Mole fraction									
H_2	9.99×10^{-1}	9.99×10^{-1}	9.99×10^{-1}	$9.99c10^{-1}$	9.99×10^{-1}	9.99×10^{-1}	9.99×10^{-1}	9.99×10^{-1}	9.99×10^{-1}
BH_2	9.20×10^{-6}	9.20×10^{-6}	9.20×10^{-6}	5.33×10^{-6}	5.33×10^{-6}	5.33×10^{-6}	4.20×10^{-6}	4.20×10^{-6}	4.20×10^{-6}
N_2	4.70×10^{-6}	4.70×10^{-6}	4.70×10^{-6}	2.81×10^{-6}	2.80×10^{-6}	2.80×10^{-6}	2.26×10^{-6}	2.25×10^{-6}	2.25×10^{-6}
NH	*	*	*	*	*	*	*	*	*
NH_2	*	*	*	*	*	*	*	*	*
N_2H_2	*	*	*	*	*	*	*	*	*
NH_3	*	2.22×10^{-10}	1.81×10^{-10}	*	7.22×10^{-10}	6.92×10^{-10}	*	1.27×10^{-9}	1.24×10^{-9}
N_2H_4	*	*	*	*	*	*	*	*	*
BH_3	2.08×10^{-7}	2.08×10^{-7}	2.08×10^{-7}	2.70×10^{-7}	2.70×10^{-7}	2.70×10^{-7}	3.01×10^{-7}	3.01×10^{-7}	3.01×10^{-7}
B(g)	*	1.90×10^{-9}	1.91×10^{-9}	*	2.20×10^{-10}	2.21×10^{-10}	*	*	*
BH	*	1.30×10^{-9}	7.85×10^{-10}	*	2.12×10^{-10}	2.04×10^{-10}	*	*	*
$B_2(g)$	*	*	*	*	*	*	*	*	*
B_2H_6	*	*	*	*	*	*	*	*	*
B_5H_9	*	*	*	*	*	*	*	*	*
$B_{10}H_{14}$	*	*	*	*	*	*	*	*	*
$B_3N_3H_6$	*	*	*	*	*	*	*	*	*
BN(g)	*	*	*	*	*	*	*	*	*
H	4.83×10^{-4}	4.83×10^{-4}	4.83×10^{-4}	2.16×10^{-4}	2.16×10^{-4}	2.16×10^{-4}	1.53×10^{-4}	1.53×10^{-4}	1.53×10^{-4}
TOTAL GAS MOLES	.0500	.5001	5.001	.0500	.5000	5.000	.0500	.5000	5.000
MOLES BN LEFT	.9999	.9999	.9999	.9999	.9999	.9999	.9999	.9999	.9999
MOLES BN ERODED	4.70×10^{-7}	4.70×10^{-6}	4.70×10^{-5}	2.81×10^{-7}	2.80×10^{-6}	2.80×10^{-5}	2.26×10^{-7}	2.25×10^{-6}	2.25×10^{-5}

*Moles less than 10^{-10}

T = 2000K

BN (1 Mole) + H_2 (1 Mole) COMPONENTS ARE H_2 AND BH_2

Table C-XV

Pressure (torr)	1.			5.			10.		
H/BN	.1	1.	10.	.1	1.	10.	.1	1.	10.
SPECIES in Mole fraction									
H_2	9.51×10^{-1}	9.51×10^{-1}	9.51×10^{-1}	9.77×10^{-1}	9.77×10^{-1}	9.77×10^{-1}	9.84×10^{-1}	9.84×10^{-1}	9.84×10^{-1}
BH_2	2.98×10^{-3}	2.98×10^{-3}	2.98×10^{-3}	1.90×10^{-3}	1.90×10^{-3}	1.90×10^{-3}	1.53×10^{-3}	1.53×10^{-3}	1.53×10^{-3}
N_2	1.96×10^{-3}	1.96×10^{-3}	1.96×10^{-3}	1.02×10^{-3}	1.01×10^{-3}	1.02×10^{-3}	7.97×10^{-4}	7.97×10^{-4}	7.97×10^{-4}
NH	*	*	6.60×10^{-11}	*	*	4.80×10^{-11}	*	*	4.25×10^{-11}
NH_2	*	5.58×10^{-10}	5.76×10^{-10}	7.46×10^{-10}	9.39×10^{-10}	9.57×10^{-10}	*	1.19×10^{-9}	1.20×10^{-9}
N_2H_2	*	*	*	*	*	*	*	*	*
NH_3	*	1.07×10^{-9}	1.10×10^{-9}	3.83×10^{-9}	4.12×10^{-9}	4.15×10^{-9}	7.12×10^{-9}	7.38×10^{-9}	7.41×10^{-9}
N_2H_4	*	*	*	*	*	*	*	*	*
BH_3	8.16×10^{-6}	3.16×10^{-6}	8.16×10^{-6}	1.18×10^{-5}	1.18×10^{-5}	1.18×10^{-5}	1.34×10^{-5}	1.34×10^{-5}	1.34×10^{-5}
B(g)	8.66×10^{-4}	8.66×10^{-4}	8.66×10^{-4}	1.07×10^{-4}	1.07×10^{-4}	1.07×10^{-4}	4.29×10^{-5}	4.29×10^{-5}	4.29×10^{-5}
BH	5.44×10^{-5}	5.44×10^{-5}	5.44×10^{-5}	1.53×10^{-5}	1.53×10^{-5}	1.53×10^{-5}	8.67×10^{-6}	8.67×10^{-6}	8.67×10^{-6}
$B_2(g)$	6.61×10^{-8}	6.61×10^{-8}	6.61×10^{-8}	5.10×10^{-9}	5.08×10^{-9}	5.08×10^{-9}	1.64×10^{-9}	1.62×10^{-9}	1.62×10^{-9}
B_2H_6	*	*	*	*	*	*	*	*	*
B_5H_9	*	*	*	*	*	*	*	*	*
$B_{10}H_{14}$	*	*	*	*	*	*	*	*	*
$B_3N_3H_6$	*	*	*	*	*	*	*	*	*
BN(g)	1.18×10^{-6}	1.18×10^{-6}	1.18×10^{-6}	2.36×10^{-7}	2.36×10^{-7}	2.36×10^{-7}	1.18×10^{-7}	1.18×10^{-7}	1.78×10^{-7}
H	4.35×10^{-2}	4.35×10^{-2}	4.35×10^{-2}	1.97×10^{-2}	1.97×10^{-2}	1.97×10^{-2}	1.40×10^{-2}	1.40×10^{-2}	1.40×10^{-2}
TOTAL MOLES GAS	.0513	.5126	5.126	.0505	.5055	5.055	.0504	.5039	.5039
MOLES BN LEFT	.9997	.9979	.9799	.9999	.9989	.9897	.9999	.9991	.9919
MOLES BN ERODED	2.01×10^{-4}	2.01×10^{-3}	2.01×10^{-2}	1.03×10^{-4}	1.03×10^{-3}	1.03×10^{-2}	8.03×10^{-5}	8.03×10^{-4}	8.03×10^{-3}

*Mole fraction less than 10^{-10}

T = 1100K

BN (1 Mole) + H (1 Mole) COMPONENTS ARE $NH_3(g)$ AND $BH_3(g)$

Table C- XVI

Pressure (torr)	1.			5.			10.		
H/BN	.1	1.	‡ 10.	.1	1.	10.	.1	1.	10.
SPECIES in Mole fraction									
H	1.23×10^{-3}	1.23×10^{-3}	1.23×10^{-3}	4.21×10^{-4}	4.21×10^{-4}	4.21×10^{-4}	2.65×10^{-4}	2.65×10^{-4}	2.64×10^{-4}
BH_3	4.96×10^{-1}	4.96×10^{-1}	4.96×10^{-1}	4.85×10^{-1}	4.85×10^{-1}	4.85×10^{-1}	4.72×10^{-1}	4.72×10^{-1}	4.72×10^{-1}
N_2	5.05×10^{-8}	5.08×10^{-8}	5.08×10^{-8}	1.01×10^{-8}	1.04×10^{-8}	1.05×10^{-8}	5.83×10^{-9}	5.48×10^{-9}	5.44×10^{-9}
NH	*	*	5.33×10^{-8}	*	*	*	*	*	*
NH_2	3.17×10^{-9}	3.30×10^{-9}	3.31×10^{-9}	*	1.94×10^{-9}	1.96×10^{-9}	*	1.59×10^{-9}	1.57×10^{-9}
N_2H_2	*	*	2.34×10^{-20}	*	*	*	3.46×10^{-10}	*	*
NH_3	5.00×10^{-1}	5.00×10^{-1}	5.00×10^{-1}	5.05×10^{-1}	5.05×10^{-1}	5.05×10^{-1}	5.09×10^{-1}	5.09×10^{-1}	5.09×10^{-1}
N_2H_4	*	*	4.11×10^{-17}	*	*	*	*	*	*
B(g)	*	*	1.19×10^{-18}	*	*	*	*	*	*
BH	*	*	4.23×10^{-14}	*	*	*	*	*	*
BH_2	6.22×10^{-4}	6.22×10^{-4}	6.22×10^{-4}	3.56×10^{-4}	3.56×10^{-4}	3.56×10^{-4}	2.76×10^{-4}	2.76×10^{-4}	2.76×10^{-4}
$B_2(g)$	*	*	3.62×10^{-31}	*	*	*	*	*	*
B_2H_6	2.07×10^{-3}	2.07×10^{-3}	2.07×10^{-3}	9.88×10^{-3}	9.88×10^{-3}	9.88×10^{-3}	1.87×10^{-2}	1.87×10^{-2}	1.87×10^{-2}
B_5H_9	*	*	5.78×10^{-16}	*	*	*	*	*	*
$B_{10}H_{14}$	*	*	4.33×10^{-32}	*	*	*	*	*	*
BN(g)	*	*	4.63×10^{-22}	*	*	*	*	*	*
$B_3N_3H_6$	3.02×10^{-7}	3.01×10^{-7}	3.01×10^{-7}	1.48×10^{-6}	1.48×10^{-6}	1.48×10^{-6}	2.92×10^{-6}	2.92×10^{-6}	2.92×10^{-6}
TOTAL GAS MOLES	.0333	.3330	3.330	.0330	.3302	3.302	.0327	.3273	3.273
MOLES BN LEFT	.9833	.8334	None	.9833	.8333	None	.9833	.8333	None
MOLES BN ERODED	.0166	.1666	1.666	.0166	.1666	1.666	.0166	.1667	1.666

*Less than 10^{-10} moles
‡ All values computed

T = 1500K

BN (1 Mole) + H (1 Mole) COMPONENTS ARE $NH_3(g)$ AND $BH_3(g)$

Table C-XVII

Pressure (torr)	1.			5.			10.		
H/BN	.1	1.	10.	.1	1.	10.	.1	1.	10.
SPECIES in Mole fraction									
H	1.92×10^{-1}	1.92×10^{-1}	1.92×10^{-1}	6.93×10^{-2}	6.93×10^{-2}	6.93×10^{-2}	4.42×10^{-2}	4.42×10^{-2}	4.42×10^{-2}
BH_3	3.66×10^{-1}	3.66×10^{-1}	3.66×10^{-1}	4.39×10^{-1}	4.39×10^{-1}	4.39×10^{-1}	4.56×10^{-1}	4.56×10^{-1}	$4.56c10^{-1}$
N_2	5.93×10^{-3}	5.93×10^{-3}	5.93×10^{-3}	1.16×10^{-3}	1.16×10^{-3}	1.16×10^{-3}	5.76×10^{-4}	5.76×10^{-4}	5.76×10^{-4}
NH	*	*	*	*	*	*	*	*	*
NH_2	6.58×10^{-6}	6.58×10^{-6}	6.58×10^{-6}	4.26×10^{-6}	4.26×10^{-6}	4.26×10^{-6}	3.44×10^{-6}	3.44×10^{-6}	3.44×10^{-6}
N_2H_2	*	*	*	3.32×10^{-10}	*	*	*	*	*
NH_3	3.95×10^{-1}	3.95×10^{-1}	3.95×10^{-1}	4.64×10^{-1}	4.64×10^{-1}	4.64×10^{-1}	4.77×10^{-1}	4.77×10^{-1}	4.77×10^{-1}
N_2H_4	*	*	*	*	*	*	*	*	*
B(g)	*	*	*	*	*	*	*	*	*
BH	1.43×10^{-8}	1.45×10^{-8}	1.45×10^{-8}	5.08×10^{-9}	5.28×10^{-9}	5.30×10^{-9}	3.18×10^{-9}	3.41×10^{-9}	3.39×10^{-9}
BH_2	4.07×10^{-2}	4.07×10^{-2}	4.07×10^{-2}	2.70×10^{-2}	2.70×10^{-2}	2.70×10^{-2}	2.20×10^{-2}	2.20×10^{-2}	2.20×10^{-2}
$B_2(g)$	*	*	*	*	*	*	*	*	*
B_2H_6	1.06×10^{-5}	1.06×10^{-5}	1.06×10^{-5}	7.58×10^{-5}	7.58×10^{-5}	7.58×10^{-8}	1.64×10^{-4}	1.64×10^{-4}	1.64×10^{-4}
B_5H_9	*	*	*	*	*	*	*	*	*
$B_{10}H_{14}$	*	*	*	*	*	*	*	*	*
BN(g)	*	*	*	*	*	*	*	*	*
$B_3N_3H_6$	2.98×10^{-8}	2.98×10^{-8}	2.99×10^{-8}	2.10×10^{-7}	2.10×10^{-7}	2.10×10^{-7}	4.49×10^{-7}	4.49×10^{-7}	4.49×10^{-7}
TOTAL GAS MOLES	.0391	.3909	3.909	.0353	.3532	.3532	.0346	.3462	3.462
MOLES BN LEFT	.9841	.8408	None	.9835	.8354	-.6458	.9834	.8344	-.6559
MOLES BN ERODED	.0159	.1592	1.592	.0164	.1645	1.646	.0166	.1656	1.656

*Less than 10^{-10} moles

T = 2000K

BN (1 Mole) + H (1 Mole) COMPONENTS H(g) AND BH_3(g)

Table C-XVIII

Pressure (torr)	1.			5.			10.		
H/BN	.1	1.	10.	.1	1.	10.	.1	1.	10.
SPECIES in Mole fraction (g)									
H	7.68×10^{-1}	7.68×10^{-1}	7.68×10^{-1}	6.50×10^{-1}	6.50×10^{-1}	6.50×10^{-1}	5.81×10^{-1}	5.81×10^{-1}	5.81×10^{-1}
BH_3	7.11×10^{-3}	7.11×10^{-3}	7.11×10^{-3}	3.95×10^{-2}	3.95×10^{-2}	3.95×10^{-2}	7.40×10^{-2}	7.40×10^{-2}	7.40×10^{-2}
N_2	7.74×10^{-2}	7.74×10^{-2}	7.74×10^{-2}	1.16×10^{-1}	1.16×10^{-1}	1.16×10^{-1}	1.35×10^{-1}	1.35×10^{-1}	1.35×10^{-1}
NH	7.35×10^{-9}	7.43×10^{-9}	7.44×10^{-9}	1.71×10^{-8}	1.72×10^{-8}	1.72×10^{-8}	2.34×10^{-8}	2.35×10^{-8}	2.35×10^{-8}
NH_2	1.13×10^{-6}	1.13×10^{-6}	1.13×10^{-6}	1.11×10^{-5}	1.11×10^{-5}	1.11×10^{-5}	2.71×10^{-5}	2.71×10^{-5}	2.71×10^{-5}
N_2H_2	*	*	*	*	*	*	*	*	*
NH_3	3.80×10^{-5}	3.80×10^{-5}	3.80×10^{-5}	1.58×10^{-3}	1.58×10^{-3}	1.58×10^{-3}	6.91×10^{-3}	6.91×10^{-3}	6.91×10^{-3}
N_2H_4	*	*	*	*	*	*	*	*	*
B(g)	1.38×10^{-4}	1.38×10^{-4}	1.38×10^{-4}	1.01×10^{-5}	1.01×10^{-5}	1.01×10^{-5}	3.30×10^{-6}	3.30×10^{-6}	3.30×10^{-6}
BH	1.52×10^{-4}	1.53×10^{-4}	1.52×10^{-4}	4.73×10^{-5}	4.73×10^{-5}	4.73×10^{-5}	2.77×10^{-5}	2.77×10^{-5}	2.77×10^{-5}
BH_2	1.47×10^{-1}	1.47×10^{-1}	1.47×10^{-1}	1.93×10^{-1}	1.93×10^{-1}	1.93×10^{-1}	2.03×10^{-1}	2.03×10^{-1}	2.03×10^{-1}
B_2(g)	1.72×10^{-9}	1.68×10^{-9}	1.67×10^{-9}	*	*	4.48×10^{-11}	*	*	*
B_2H_6	*	1.59×10^{-10}	1.89×10^{-10}	2.92×10^{-8}	2.95×10^{-8}	2.96×10^{-8}	2.08×10^{-7}	2.08×10^{-7}	2.08×10^{-7}
B_5H_9	*	*	*	*	*	*	*	*	*
$B_{10}H_{14}$	*	*	*	*	*	*	*	*	*
BN(g)	1.18×10^{-6}	1.18×10^{-6}	1.18×10^{-6}	2.36×10^{-7}	2.36×10^{-7}	2.36×10^{-7}	1.18×10^{-7}	1.18×10^{-7}	1.18×10^{-7}
$B_3N_3H_6$	*	*	*	*	*	1.77×10^{-11}	*	3.14×10^{-10}	3.46×10^{-10}
TOTAL GAS MOLES	.0922	.9223	9.223	.0862	.8622	8.622	.0813	.8132	8.132
FRACTION BN LEFT	.9858	.8571	None	.9799	.7992	None	.9775	.7749	None
MOLES BN ERODED	.0142	.1429	1.429	.0201	.2008	2.008	.0225	.2250	2.250

*Less than 10^{-10} moles

TABLE C-XIX

T = 1100K	SiC (1 Mole) + H (1 Mole) COMPONENTS ARE SiH_4 (g) AND CH_4 (g)
Pressure (torr)	1.
H/SiC	1.
Species in Mole Fraction	
H	6.82×10^{-5}
CH_4	4.99×10^{-1}
SiH_4	4.99×10^{-1}
SiH	1.32×10^{-8}
Si	1.17×10^{-10}
Si_2	2.22×10^{-14}
Si_3	8.82×10^{-15}
SiC_2	1.13×10^{-48}
Si_2	7.65×10^{-33}
SiC (g)	4.64×10^{-25}
CH	1.49×10^{-23}
CH_2	7.97×10^{-17}
CH_3	4.28×10^{-8}
C_2H_2	2.21×10^{-12}
C_2H	0.0
C_2H_2	1.10×10^{-18}
C_2H_4	1.55×10^{-9}
Total Moles of Gas	.2500
Moles SiC Remaining	.8750
Moles SiC Eroded	.1250

TABLE C-XX

THE PRESSURE DEPENDENTS OF THE REACTION BeO + H

T = 1100K

H/BeO = 1

Pressure (torr)	.01	.001	.0001	.00001
Species (Mole Fract.)				
H	2.92×10^{-1}	6.50×10^{-1}	9.29×10^{-1}	9.92×10^{-1}
H_2O	$3.54 \times 10^{-}$	1.75×10^{-1}	3.57×10^{-2}	4.07×10^{-3}
BeH	8.54×10^{-9}	1.89×10^{-8}	2.70×10^{-8}	2.88×10^{-8}
BeOH	2.63×10^{-10}	5.87×10^{-10}	8.67×10^{-10}	9.24×10^{-10}
BeH_2	3.54×10^{-1}	1.75×10^{-1}	3.57×10^{-2}	4.07×10^{-3}
$Be(OH)_2$	4.72×10^{-8}	2.33×10^{-8}	4.83×10^{-9}	5.98×10^{-10}
Be_2O	*	*	*	*
OH	*	*	*	*
Be	8.50×10^{-9}	8.04×10^{-9}	8.00×10^{-8}	7.99×10^{-7}
O_2	*	*	*	*
BeO (g)	*	*	*	*
BC_2O_2	*	*	*	*
Be_3O_3	*	*	*	*
Be_4O_4	*	*	*	*
Be_5O_5	*	*	*	*
Be_6O_6	*	*	*	*
O	*	*	*	*
(Moles Gas) Total	5.86×10^{-1}	7.41×10^{-1}	9.33×10^{-1}	9.92×10^{-1}
Moles BeO Remaining	7.93×10^{-1}	8.70×10^{-1}	9.67×10^{-1}	9.96×10^{-1}
Moles BeO Eroded	2.07×10^{-1}	1.29×10^{-1}	3.33×10^{-2}	4.04×10^{-3}

*Moles less than 10^{-10}

ALT:110(80)